FREE FLEXURAL AND TORSIONAL VIBRATIONS OF A SHAFT LOADED AND SUPPORTED PERIODICALLY

A Thesis Submitted
in Partial fulfilment of the Requirements
for the Degree of
MASTER OF TECHNOLOGY

By
LT. SIBA KUMAR PATNAIK

to the
DEPARTMENT OF MECHANICAL ENGINEERING
INDIAN INSTITUTE OF TECHNOLOGY, KANPUR
JULY, 1981

ME-1981-M-PAT-FRE

CERTIFICATE

This is to certify that the thesis entitled "Free Flexural and Torsional Vibrations of a Shaft Loaded and Supported Periodically" is a record of work carried out under my supervision and that it has not been submitted elsewhere for the award of a degree.

A. K. Mallik
Assistant Professor
Department of Mech. Engg.
Indian Institute of Technology
Kanpur

July 1981.

ACKNOWLEDGEMENT

I take this opportunity to express my sincere gratitude and thanks to Dr. A.K. Mallik for his valuable guidance and constant encouragement throughout the course of this work.

I would like to express my hearty thanks to E.S. Reddy, Himanshu Hatwal and LT. A.K. Tiwari for their co-operation and valuable assitance from time to time.

Thanks are also due to Mr. L.S. Bajpai, Mr. Verma and Mr. Tripathi for their sincere effort to produce the work in the present form.

Lieut. S.K. Patnaik

CONTENTS

LIST OF FIGURES

LIST OF TABLES

NOMENCLATURE

A	–	Area of cross-section of the shaft
A's, B's C's, D's	–	Constants in the solutions of differential equations
C_b	–	$\sqrt{EI/\rho A}$
C_t	–	$\sqrt{G/\rho}$
D	–	Diameter of the disc
d	–	Diameter of the shaft
E	–	Young's modulus of the material
F_A, F_B F_P, F_Q	–	Harmonic forces at the respective ends
G	–	Shear modulus of the material
I	–	Moment of inertia (in bending) of cross-section of the shaft
I_D	–	Mass moment of inertia of the disc
I_p	–	Polar moment of inertia of cross-section of the shaft
I_s	–	Mass moment of inertia of the shaft
k_1	–	Wave number $(= \frac{\omega}{C_t} l)$
k_2	–	Wave number $(k_2^4 = \omega^2 l^4 / C_b^2)$
k_r	–	Rotational stiffness in flexure at the support
$\bar{k}_r$	–	Non-dimensional rotational stiffness $(=k_r l/EI)$
k_t	–	Transverse stiffness at the supports
$\bar{k}_t$	–	Non-dimensional transverse stiffness $(= k_t l^3/EI)$
L, l	–	Length of the span
M	–	Bending moment

M_b	-	Mass of the beam
m	-	Integer
N	-	Number of bays
n	-	Number of discrete inertias/masses
q_A, q_B	-	Generalised harmonic displacements at the respective ends
q_{P+}, q_{P-}		
q_{Q+}, q_{Q-}		
t	-	Time
U's	-	Quantities defined in Appendix - C
$\bar{W}$	-	Non-dimensional transverse displacement of the beam
W	-	Solution of the beam differential equation
x	-	Length co-ordinate

Greek Symbols

α, β, γ, δ	-	Receptance functions (Appendix - D)
β_{AA}, β_{BB}	-	Direct receptance functions
β_{AB}, β_{BA}	-	Cross receptance functions
β_{c+}, β_{c-}	-	Characteristic receptance function of positive and negative going wave respectively
ρ	-	Density of the shaft material
θ	-	Angular displacement of the shaft
Ω_b	-	Non-dimensional bending frequency $\left(= \frac{\sqrt{M_b l^3}}{EI} \cdot \omega\right)$
Ω_s	-	Non-dimensional torsional frequency $(= k_1)$
ω	-	Frequency

ξ	-	Non-dimensional length co-ordinate
μ	-	Propagation constant
$\mu_{r,b}$, $\mu_{r,t}$	-	Real part of propagation constant in bending and torsion respectively
$\mu_{i,b}$, $\mu_{i,t}$	-	Imaginary part of propagation constant

Subscripts

b	-	Beam/bending
i	-	Imaginary part
r	-	Real part
s	-	Shaft
t	-	Torsion

SYNOPSIS

Flexural and torsional natural frequencies of a shaft, which is loaded and supported periodically, are investigated in this thesis. The analysis is carried out by using a 'wave approach'. In this approach, first the free harmonic wave propagation, both in torsion and in flexure, in an otherwise identical infinite shaft is studied. The results are then utilized to compute the natural frequencies of the finite shaft. This method renders the computational effort independent of the number of spans in the shaft.

By proper choice of parameters, it is shown that operating speed ranges, free from both bending and torsional resonances, can be obtained. Suggestions for widening such speed ranges of operation are also included.

CHAPTER 1

INTRODUCTION

1.1 Introduction

Most of the marine vessels use steam and gas turbines for both propulsion and power generation. In these, the shafts for transmitting power need a safe speed range of operation without any resonance. It is also important to know the vibration characteristics of a ship's diesel installation consisting of a stepped shaft on multiple supports with a series of discrete inertias. Furthermore, there are instances where the shaft rigidity is of primary consideration as compared to its strength, e.g., the cam-shaft in various engines. These shafts are also provided with a large number of supports in order to minimise the shaft deflection. This is essential for proper functioning of the cam-follower system.

All these shafts may be excited by loads which generate vibration both in torsional and flexural modes. These vibrations, if excessive, may give rise to mal-functioning and even fatigue failure in some cases. A shaft with too many lumped inertias has closely clustered torsional natural frequencies. Likewise, a shaft on a large number of supports has closely clustered flexural natural frequencies. The number of frequencies in every cluster depends on the number of lumped inertias and the supports,

respectively. Moreover, the bending and the torsional natural frequencies may also overlap. All these result in a very narrow range of operating speeds for such shafts. Hence, while designing these shafts, it is essential to have an accurate knowledge of all the natural frequencies.

To this end, as a first choice to a designer, the shaft may be idealised as one loaded and supported periodically. After determining the natural frequencies the study can be oriented towards an attempt to put the bending and the torsional natural frequencies in a narrow range. This, if achieved, may result in a wider range for the operating speed.

1.2 Short Review of Previous Work

Extensive work is reported on finding the torsional frequencies of crank shafts of multi-cylinder engines [1,2] where crank shafts are idealised as lumped rotors connected by inertialess shafts. Such a model is accurate as long as the shaft inertia is reasonably smaller than the smallest inertia of the rotors [3]. Natural frequencies of a heavy shaft, e.g., that of a heavy marine engine with rotors, were developed by Lewis [4]. He developed a graphical technique of finding out the frequencies of a single-mass elastic system and later, extended his method to systems of several degrees of freedom. The frequency equation for the special case of a single shaft with rotors at either end is available in Ref. [5], while for the general case, a hand-computational

method is outlined by Ker Wilson [1]. In reference [1], the torque summation for a system performing free torsional vibration put equal to zero for finding out the exact natural frequencies. The difficulties often encountered with the torque summation method (Holzer's method) are (1) in estimating the initial value of ω^2, and (2) in selecting the second trial value of ω^2 if the initial trial value does not satisfy the torque summation equation. The estimation of the initial trial value depends on judgement and experience, but reasonable trial values for the lower modes can be obtained by reducing the multi-disc system to a two- or three-disc systems. Grouping together discs that have shafts with relatively high stiffness between them, or neglecting discs with inertias that are small compared to the other discs, however, would give a fair approximation.

Maltbaek [6,7] studied free torsional vibrations of a stepped shaft with a series of discrete inertias and torsional springs acting on the shaft. In this analysis, a determinant of order (2nx2n) is solved to obtain the natural frequencies, where n is the number of discrete inertias. He also described [6] in detail the influence of a discrete inertia (its value and position) on the free torsional vibration of a uniform shaft with torsionally elastic end constraints. Rao [8] derived a simple n^{th} order frequency determinant to compute the frequencies and modes of an n stepped shaft with rotors. As an example, the method was used to find the frequencies and modes of a

heavy homogeneous engine in which the effect of shaft inertia was shown to be small for higher modes. Natural frequencies of such systems decrease linearly with the shaft inertia parameter when the shaft is very heavy.

It is seen from the above literature that the analysis of long shafts with too many rotors becomes cumbersome and unwieldy by the conventional methods. If the shaft is loaded periodically, a 'wave approach' can, however, be used profitably. In this method, the amount of computation remains independent of the number of lumped inertias. In the case of flexural vibration of periodically-supported beams, wave propagation theory has been applied to find the modes and natural frequencies [9-14].

The concept of wave propagation in periodically-supported, undamped structures was introduced by Heckl [9,10]. Later Mead [11] analysed the free harmonic wave propagation in an infinite beam supported periodically by both rigid and flexible supports. He obtained distinct attenuation and propagation zones of free wave motion in such a beam. Using this wave approach, Sengupta [12] reported a graphical method of finding natural frequencies of periodically-supported finite beams with different end conditions.

1.3 Objective and Scope of the Present Work

The major objective of the present work is to study harmonic torsional wave propagation in an infinite shaft with periodic rotors, taking into account of the inertia of the

shaft. The rotors are idealised as circular discs. The discs and shafts are assumed to be of the same material. The complex propagation constant for such a shaft is obtained as a function of frequency. Alternate propagation and attenuation bands of the free wave motion is plotted against the frequency. From these plots, natural frequencies of finite shafts are obtained.

Next, to consider the bending vibration of such a periodically loaded shaft, it is assumed that the shaft is supported by identical, equi-distant bearings. Furthermore, only one rotor is supposed to be located between two consecutive bearings. Short bearings are idealised as line supports whereas long bearings are considered to provide rotational constraints to the bending vibration. Initially, all the bearings are considered to be rigid so far as transverse oscillation is considered. The bending natural frequencies are also obtained by using the wave approach [13].

In the third phase, an attempt is made to match the groups of bending and torsional frequencies as far as possible. To this end, a parametric investigation is carried out by varying the parameters L/d, D/d, ξ_f and $\bar{k}_r$; where L is the bearing spacing, D and d refer respectively, to the disc and shaft diameters, ξ_f represents non-dimensional distance of the disc from the adjacent bearing on the left and $\bar{k}_r$ indicates the non-dimensional rotational stiffness

of the bearing. With a good matching of these clusters of bending and torsional frequencies, a wider operating speed range for the shaft could be available. In such a range the shaft will be free from both bending and torsional oscillations.

At the end, a short discussion is also added wherein the bearingsare considered to be flexible in the transverse direction. No detailed analysis with flexible bearings is included in the present work. The practical limitation of such an idealised shaft which is both loaded and supported periodically should be kept in mind. However, the results obtained from the analysis presented in the thesis can act as a good guide to a designer for his first choice.

CHAPTER 2

FREE TORSIONAL AND BENDING VIBRATION OF A SHAFT LOADED AND SUPPORTED PERIODICALLY

2.1 Theory of Harmonic Wave Propagation

2.1.1 The concept of wave propagation

In an infinite shaft or beam type periodic structures, harmonic waves can propagate freely (without decaying) in certain frequency ranges called propagation zones. Frequencies outside these propagation zones are called attenuation zones. In these zones, a wave once started will decay as it spreads outwards. The complex propagation constant, μ which characterises the wave motion is the measure of the rate of decay and the change of phase of the wave motion over the distance between adjacent supports. There always exist positive and negative propagation constants ($\pm \mu$). The negative sign in front of the complex number implies that the wave is propagating, or decaying, from left to right and the positive sign implies the reverse direction. The propagation constant is a function of frequency and system parameters.

2.1.2 Evaluation of propagation constants

A periodic system consists of a number of identical elements, E, each having a single coupling co-ordinate with respect to its neighbour at either ends (Fig. 2.1(a)). Such a system is referred to as a mono-coupled system. Each element E is characterised by its receptances, which relate

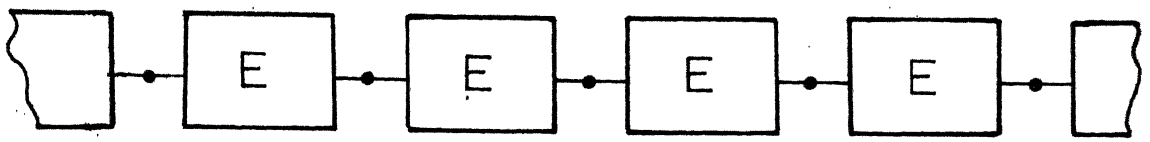

(a)

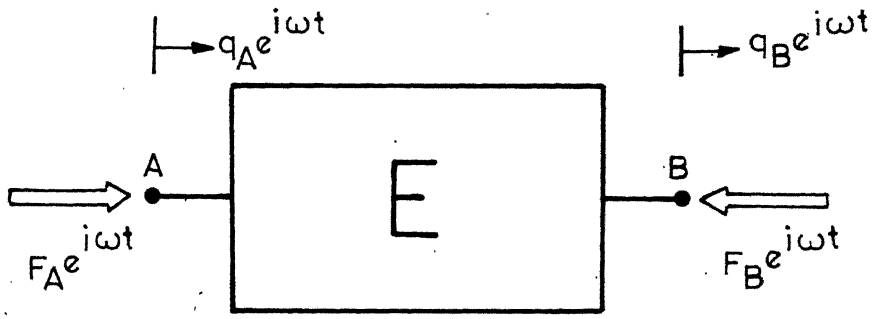

(b)

FIG. 2.1 (a) BLOCK DIAGRAM OF A SYSTEM OF MONOCOUPLED ELEMENTS

FIG. 2.1 (b) FORCES ON, AND DISPLACEMENTS OF A SINGLE ELEMENT

the harmonic displacements at the coupling co-ordinates to the harmonic forces at those co-ordinates. Let the harmonic displacements at the left and right hand coupling co-ordinates of a single element be $q_A \exp(i\omega t)$ and $q_B \exp(i\omega t)$ and the harmonic forces acting opposite to one another at these co-ordinates be $F_A \exp(i\omega t)$ and $F_B \exp(i\omega t)$, respectively (Fig. 2.1(b)). The displacements and forces are related as follows through the receptance matrix $[\beta]$:

$$\begin{Bmatrix} q_A \\ q_B \end{Bmatrix} = \begin{bmatrix} \beta_{AA} & \beta_{AB} \\ \beta_{BA} & \beta_{BB} \end{bmatrix} \cdot \begin{Bmatrix} F_A \\ F_B \end{Bmatrix} \qquad (2.1)$$

where β_{ij} is the harmonic displacement at co-ordinate i due to a unit harmonic force at co-ordinate j. The receptances β_{ij}'s are functionsof frequency and the element characteristics.

If an infinite number of elements like 'E' are coupled together, free motion of the system is possible when the following recurrence relationship holds good for every element:

$$q_B = e^{\mu} q_A \qquad (2.2)$$

$$F_B = e^{\mu} F_A \qquad (2.3)$$

For a linear system $\beta_{AB} = -\beta_{BA}$, so that there are three significant receptances. Further, for a symmetric element these reduce to two as $\beta_{AA} = -\beta_{BB}$.

Using Eqns. 2.2 and 2.3 , the pair of equations 2.1 become

$$q_A = (\beta_{AA} + e^{\mu} \beta_{AB}) F_A \qquad (2.4)$$

and $$e^{\mu} q_A = (\beta_{BA} + e^{\mu} \beta_{BB}) F_A \qquad (2.5)$$

For non-trivial solution of, F_A and F_B, in case of a linear system, one gets

$$\beta_{AA} - \beta_{BB} + (e^{\mu} + e^{-\mu}) \beta_{AB} = 0 \qquad (2.6)$$

hence $$\cosh \mu = \frac{(\beta_{BB} - \beta_{AA})}{2\beta_{AB}} \qquad (2.7)$$

Eqn. 2.6 simplifies to a quadratic equation in e^{μ} as

$$e^{2\mu} + [(\beta_{AA} - \beta_{BB})/\beta_{AB}] e^{\mu} + 1 = 0 \qquad (2.8)$$

the solution of which is

$$e^{\mu_{1,2}} = r \pm \sqrt{r^2 - 1} \qquad (2.9)$$

where $$r = (\beta_{BB} - \beta_{AA})/2\beta_{AB} = \cosh \mu \qquad (2.10)$$

2.1.3 Dependency of propagation constant on frequency

Considering an undamped periodic system, the term r in Eqn. 2.10 is entirely real and varies between $\pm\infty$ as the frequency is varied. If it is greater than + 1, μ is entirely real (μ_r) and there is a constant exponential rate of decay of the wave motion from one element to the next. Since μ has no imaginary part, there is no phase difference

between the motion in adjacent elements and the wave is of non-propagating form. If r is less than -1, then μ has the form $\mu_r+i\pi$, the imaginary part implies that adjacent elements vibrate exactly in counter-phase and the wave is still of non-propagating type. These frequency ranges, for which $\mu_r \neq 0$, are called attenuation zones. On the other hand, if r is real and is between -1 and +1, μ is entirely imaginary ($i\mu_i$) which implies non-zero phase difference between the motions in adjacent elements, so that the wave is now propagating. There is no decay of the wave motion between successive elements as the real part of μ is zero. The frequency ranges for which $\mu_r = 0$ are referred to as propagation zones.

2.1.4 Natural frequencies of finite periodic systems

Wave propagation can occur provided μ is imaginary, and this occurs when $-1 \leqslant \cosh \mu \leqslant +1$. Thus the bounds of the frequency in which wave propagation takes place are governed by

$$\cosh\mu = (\beta_{BB} - \beta_{AA})/2\beta_{AB} = \pm 1 \qquad (2.11)$$

For a symmetric element, $\beta_{AA} = -\beta_{BB}$, so that $\cosh \mu = -\beta_{AA}/\beta_{AB}$. The bounding frequencies of the propagation bounds in this case are therefore that at which $\beta_{AA} = \mp \beta_{AB}$.

Let us consider a single system element, disconnected from its neighbours, so that its ends are free. At its natural frequencies the receptances have infinite values,

but the ratios β_{AA}/β_{BB} and β_{AA}/β_{AB} remain finite and determinate. In particular, for a symmetric element they become -1 and ± 1, respectively, the sign of the later depending on the nature of the system and the mode. Hence at the natural frequencies of the free symmetric element, the finite receptance ratios make cosh μ for the periodic system equal to ± 1.

If the same single element is locked at both of its ends, it has different natural frequencies. These are obtained from the pair of following equations :

$$q_A = \beta_{AA} F_A + \beta_{AB} F_B \qquad 2.12(a)$$

$$q_B = \beta_{BA} F_A + \beta_{BB} F_B \qquad 2.12(b)$$

For a locked element, $q_A = q_B = 0$ and the natural frequencies are the roots of the determinant equation

$$\begin{vmatrix} \beta_{AA} & \beta_{AB} \\ \beta_{BA} & \beta_{BB} \end{vmatrix} = 0 \qquad (2.13)$$

As mentioned earlier, for a symmetric element putting $\beta_{BA} = -\beta_{AB}$, and $\beta_{AA} = -\beta_{BB}$ equation 2.13 reduces to

$$\beta_{AB}^2 - \beta_{AA}^2 = 0$$

or

$$\beta_{AA}/\beta_{AB} = \pm 1 \qquad (2.14)$$

At the frequencies which satisfy Eqn. 2.14 (the natural frequencies), cosh μ is again found to be ± 1. It follows, then, that the bounding frequencies of a periodic system of

symmetric elements (at which $\cosh \mu = \pm 1$) are also natural frequencies of the single element with either free ends or locked ends.

If the element is unsymmetric, $\beta_{AA} \neq -\beta_{BB}$. However, the natural frequencies of the locked element are still the roots of Eqn. 2.13 and this may be expressed in the form

$$\beta_{AA}/\beta_{AB} = -\beta_{AB}/\beta_{BB} \qquad (2.15)$$

Hence, at these frequencies

$$\cosh \mu = (\beta_{BB} - \beta_{AA})/2\beta_{AB}$$

$$= \tfrac{1}{2} [-(\beta_{AA}/\beta_{AB}) - (\beta_{AB}/\beta_{AA})]$$

But $\cosh \mu = \frac{1}{2} (e^{\mu} + e^{-\mu})$, and so $e^{\mu} = -\beta_{AA}/\beta_{AB}$ or $-\beta_{AB}/\beta_{AA}$. These both have real values and for the general unsymmetric element, are not equal to ± 1 at the natural frequencies. Hence, μ must have a non-zero real part and the natural frequencies of the locked, unsymmetric element must lie in the attenuation zones.

In case of a single unsymmetric element with free ends, it can be shown [13] that at its natural frequencies, $\beta_{AA}\ \beta_{BB} = -\beta_{AB}^2$. Once again, then, at the natural frequencies $\beta_{AA}/\beta_{AB} = -\beta_{AB}/\beta_{BB}$ and so these frequencies must lie in attenuation zones. Hence the natural frequencies of both free and locked unsymmetric elements lie in attenuation zones and do not coincide with the bounding frequencies.

Considering a system of positive-definite elements, it can be proved that as the frequency approaches zero, propagation cannot occur, i.e. the lowest frequency range is an attenuation zone. Propagation begins at (or just above) the lowest natural frequency of the positive-definite element, which is free at its ends. If the ''free'' and ''locked'' natural frequencies of the single symmetric element occur alternately (as for certain uniform beam elements) the free natural frequencies constitute the lower frequency bounds to the propagation zones, whereas the locked frequencies constitute the upper frequency bounds [13].

If the system is semi-definite, propagation does occur as the frequency approaches zero, i.e. the lowest frequency range is a propagation zone. Propagation ceases at (or just below) the lowest of the natural frequencies of the semi-definite element with its ends either free or locked. This frequency is therefore an upper bound frequency.

Now we consider a finite mono-coupled periodic system of N elements being excited by the force F_p at the left end P (Fig. 2.2). Since the system is mono-coupled, the total motion generated can be represented by a single positive-going characteristic wave and a single negative-going wave. If the contributions to the total displacement at P from these two waves are q_{p+} and q_{p-} respectively, then

$$q_p = q_{p+} + q_{p-} \qquad (2.16)$$

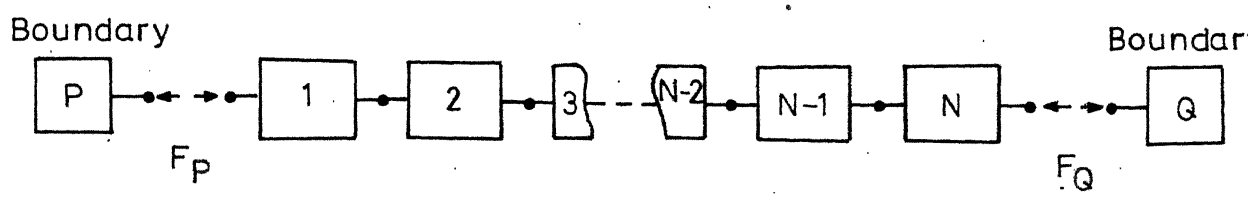

FIG·2·2 BLOCK DIAGRAM OF A FINITE PERIODIC SYSTEM OF N ELEMENTS AND ARBITRARY BOUNDARIES

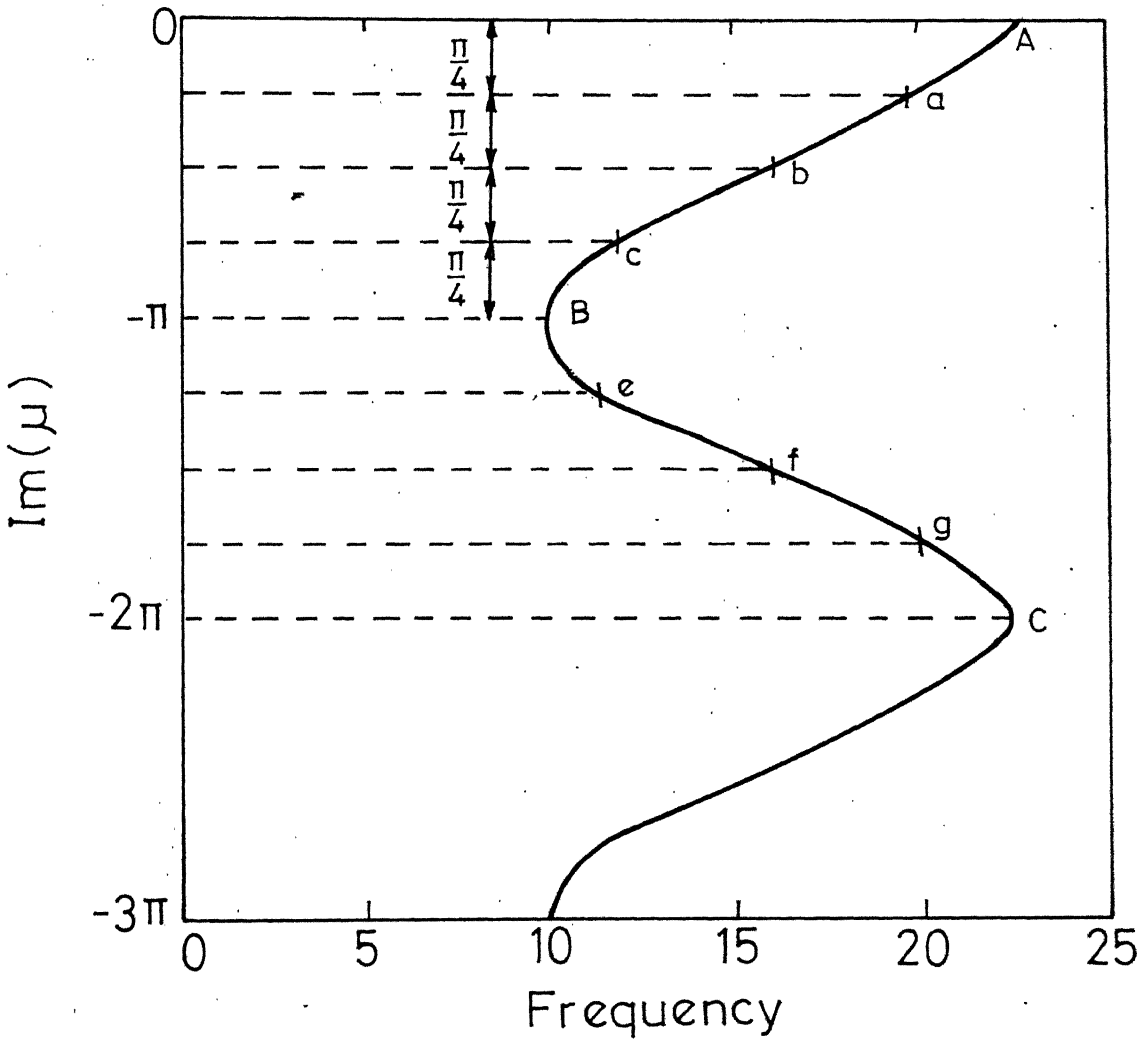

FIG·2·3 THE MULTIVALUED PROPAGATION CONSTANT CURVES VERSUS FREQUENCY

At the boundary Q the displacement of the positive wave is

$$q_{Q+} = q_{P+}\, e^{-N\mu}$$

and that for the negative wave is

$$q_{Q-} = q_{P-}\, e^{N\mu}$$

Thus, the total displacement at Q is

$$q_Q = q_{Q+} + q_{Q-} = q_{P+}\, e^{-N\mu} + q_{P-}\, e^{N\mu} \quad (2.17)$$

Defining the characteristic wave receptance (β_w) as the harmonic response at one of the coupling co-ordinates per unit internal harmonic force at that co-ordinate one gets from Eqn. 2.4

$$\beta_w = q_R/F_R = \beta_{AA} + e^{\mu}\, \beta_{AB} \quad (2.18)$$

Hence, the characteristic receptances of positive and negative going waves are, respectively, given by

$$\beta_{w+} = \beta_{AA} + e^{-\mu}\, \beta_{AB} \quad 2.19(a)$$

and

$$\beta_{w-} = \beta_{AA} + e^{\mu}\, \beta_{AB} \quad 2.19(b)$$

The total force at each end of the system shown in Fig. 2.2 is given by

$$F_P = q_{P+}/\beta_{w+} + q_{P-}/\beta_{w-} \quad 2.20(a)$$

and

$$F_Q = q_{P+}\, e^{-N\mu}/\beta_{w+} + q_{P-}\, e^{N\mu}/\beta_{w-} \quad 2.20(b)$$

Supposing that the system is free at end Q such that $F_Q = 0$, equation 2.20(b) then yields

$$q_{P-} = -(\beta_{w-}/\beta_{w+})\, q_{P+}\, e^{-2N\mu} \qquad (2.21)$$

On substituting this, and Eqns. 2.19(a) and 2.19(b), into Eqn. 2.20(a) the direct receptance at end P is found to be

$$\beta_{PP} = q_P/F_P = \beta_{AA} - \beta_{AB}\,[\sinh(N-1)\mu/\sinh N\mu] \qquad \ldots. \ 2.22(a)$$

or $$\beta_{PP} = \beta_{AA} - \beta_{AB}\,[\cosh\mu - \cosh N\mu \sinh\mu/\sinh N\mu] \qquad \ldots. \ 2.22(b)$$

The transfer receptance, $\beta_{QP} = -\beta_{PQ}$, is likewise found to be

$$\beta_{QP} = q_Q/F_P = \beta_{AB}\,[\sinh\mu/\sinh N\mu] \qquad (2.23)$$

These two receptances are entirely real, whether μ is real or imaginary, i.e. whether the frequency is in a propagation zone or in an attenuation zone. The natural frequencies of the system which is free at both ends P and Q are those frequencies at which $\beta_{PP} \longrightarrow \infty$. These occur (a) when $\beta_{AA} \longrightarrow \infty$ and (b) when $\sinh\mu/\sinh N\mu \longrightarrow \infty$. Condition (a) occurs in general, in an attenuation zone but will occur at the bound of a propagation zone if the element is, symmetric. Condition (b) can only occur in a propagation zone, for then μ is purely imaginary ($i\mu_i$) and $\sinh\mu/\sinh N\mu = \sin\mu_i/\sin N\mu_i$. This becomes

infinite, whenever $\mu_i N = m\pi$, provided $\mu_i \neq 0$ or $\pm \pi$. It has been shown [12] that the integer m is not equal to zero nor a multiple of N, i.e. $1 \leqslant m < N$, giving (N-1) discrete values of μ_i and correspondingly (N-1) discrete natural frequencies in the propagation band.

Figure 2.3 shows the imaginary part of μ (μ_i) plotted against frequency for the first propagation band of a multi-supported uniform beam. μ_i is a multi-valued function of frequency since $\mu_i = \cos^{-1} [(\beta_{BB} - \beta_{AA})/2\beta_{AB}]$. It follows that each section of the curve between $\mu_i = 0$ and π is a mirror image of the section above it.

Let the finite system has four elements. It will resonate at the frequencies given by $\mu_i = m\pi/4$ ($m \neq 0$ or a multiple of 4) and these are the frequencies of the points marked a, b, c in Fig. 2.3 for m = 1, 2, 3 and the points marked e, f, g for m = 5, 6, 7 etc. Since BC is the mirror image of BA, the frequencies of the points a and g, b and f, and c and e, respectively, are identical. Thus it can be concluded that a finite periodic system with free ends and consisting of N mono-coupled unsymmetric, positive-definite elements has N-1 natural frequencies in each propagation band, corresponding to the frequencies at which $\mu_i = m\pi/N$ (m = 1 to N-1). Close to, but just below each propagation band there is another natural frequency, corresponding to $\beta_{AA} \longrightarrow \infty$.

When the finite system with N elements is fixed at the right-hand end such that $q_Q = 0$, the direct receptance at

the left-hand end is given by

$$\beta_{PP} = \frac{(\beta_{AB}^2 - \beta_{AA}\,\beta_{BB})}{\beta_{AA} - \beta_{AB}\,\sinh\,(N+1)\,\mu/\sinh\,N\mu} \qquad (2.24)$$

The natural frequencies of a system oscillating in fixed-fixed mode (for which $\beta_{PP} = 0$) are those at which either (a) $(\beta_{AB}^2 - \beta_{AA}\,\beta_{BB}) = 0$ or, (b) $\sinh N\mu = 0$, provided $\sinh(N+1)\mu \neq 0$. Condition (a) is the equation for the natural frequencies of the single element, fixed at both ends (Eqn. 2.13). For a system of general unsymmetric elements these frequencies lie outside the propagation bands. If the elements are symmetric, they coincide with the upper boundary frequencies of the propagation zones. Condition (b) can only be satisfied in a progapation band at those frequencies for which $\sinh N\mu = \sin N\mu_i = 0$ and $\sin (N+1)\,\mu_i \neq 0$, i.e. $\mu_i = m\pi/N$, m = 1 to (N-1). Hence, these are the same (N-1) natural frequencies already discussed for the 'free-free' system, within each propagation zone.

2.2 Evaluation of Receptances for a Periodic Shaft Element

Figure 2.4 shows a periodic shaft element of length l with a disc of moment of inertia I_D at $\xi_j = \xi_{j1}$, where $\xi_j = \frac{x}{l}$ with x representing the distance of the disc from end A.

The equation of motion for the shaft is given by

$$c_t^2 \cdot \frac{\partial^2\theta}{\partial x^2} - \frac{\partial^2\theta}{\partial t^2} = 0 \qquad (2.25)$$

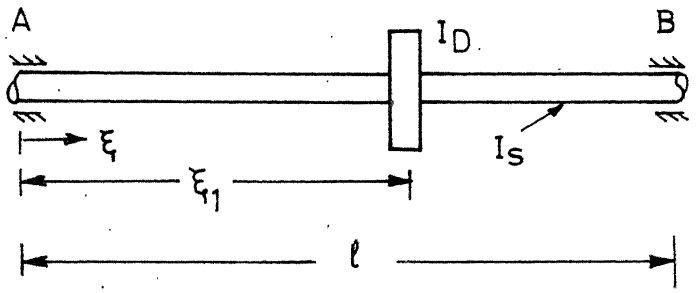

FIG·2·4 PERIODIC SHAFT ELEMENT

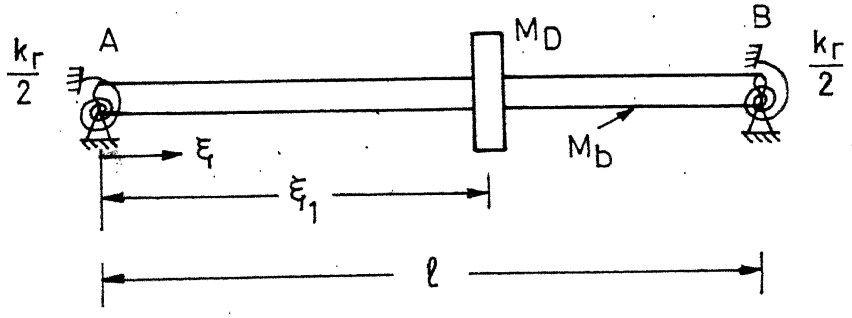

FIG·2·5 PERIODIC BEAM ELEMENT

where $c_t^2 = G/\rho$ with G and ρ as the shear modulus and the density of the shaft material respectively, and θ is the angular displacement of the shaft.

For harmonic motion, the solution of the differential equation (2.25) can be written as

$$\Theta(x) = A \cos(\omega/c_t)\, x + B \sin(\omega/c_t)\, x \qquad (2.26)$$

where ω is the frequency of oscillation and A and B are the constants to be evaluated. Using the non-dimensional coordinate ξ, Eqn. 2.26 is written as

$$\Theta = A \cos k_1\xi + B \sin k_1\xi \qquad (2.27)$$

where $k_1 = \frac{\omega}{c_t} l$ = non-dimensional torsional frequency Ω_s.
The above differential equation can be solved in two parts:

$$\Theta_L = A_1 \cos k_1\xi + B_1 \sin k_1\xi \qquad 0 < \xi \leq \xi_1$$
$$\text{and} \quad \Theta_R = A_2 \cos k_1\xi + B_2 \sin k_1\xi \qquad \xi_1 \leq \xi < 1 \qquad (2.28)$$

The constants A_1, B_1 and A_2, B_2 are obtained from the following four boundary conditions:

(i) non-dimensional torque at end A is unity,

i.e. at $\xi = 0$ $\quad \Theta'_L = 1$ 2.29(a)

(ii) torque at end B is zero which gives

at $\xi = 1$ $\quad \Theta'_R = 0$ 2.29(b)

(iii) considering continuity of angular displacement at

$\xi = \xi_1$

$\Theta_L(\xi_1) = \Theta_R(\xi_1)$ 2.29(c)

(iv) for the torque balance at the disc

$$\text{at } \xi = \xi_1, \quad \theta'_L - \theta'_R = I_D/I_s \cdot \Omega_s^2 \cdot \theta_{L/R} \qquad 2.29(d)$$

where I_D is the mass moment of inertia of the disc, and I_s is the mass moment of inertia of the shaft and is equal to $\rho I_p l$ with I_p as the polar moment of inertia of the shaft cross-section.

The (4x4) matrix equation resulting from the use of the above boundary conditions is given in Appendix-A. From the above set of equations, the constants A's and B's are evaluated and the receptance β_{AA} is obtained as θ_A.

Similarly, when unit torque is applied at end B (with end A free) the receptances β_{BB} and β_{AB} are obtained as θ_B and θ_A respectively. Using the above receptances, the propagation constant versus frequency (Ω_s) curve is obtained using Eqn. 2.9 and the plots are discussed in the next chapter.

2.3 Evaluation of Receptances for a Periodic Beam Element

Figure 2.5 shows a periodic beam element of length l with a mass M_D at $\xi = \xi_1$, where $\xi = x/l$ with x representing the distance of the disc from end A, k_r indicates the rotational stiffness of the supports.

The equation of motion for the beam is given by

$$c_b^2 \frac{\partial^4 w}{\partial x^4} + \frac{\partial^2 w}{\partial t^2} = 0 \qquad (2.30)$$

where $c_b^2 = \frac{EI}{\rho A}$ with E and I as the modulus of elasticity and area moment of inertia of the beam, respectively, ρ is

the density of beam material, A is the area of cross-section of the beam and w is the transverse displacement of the beam.

For harmonic motion, the solution of the differential equation 2.30 can be written in the non-dimensional form as

$$\bar{W}(\xi) = A_1 \cos k_2\xi + B_1 \sin k_2\xi + C_1 \cosh k_2\xi + D_1 \sinh k_2\xi \qquad (2.31)$$

where $k_2^4 = \frac{\omega^2}{c_b^2} l^4$ = square of the non-dimensional bending frequency, Ω_b^2, $\bar{W}$ is the non-dimensional transverse displacement $= (w/L)/e^{i\omega t}$, ω is the frequency of oscillation with A_1, B_1, C_1 and D_1 as the constants to be evaluated. The above differential equation can be solved in two parts :

$$\bar{W}_L = A_1 \cos k_2\xi + B_1 \sin k_2\xi + C_1 \cosh k_2\xi + D_1 \sinh k_2\xi \qquad 0 < \xi \leq \xi_1$$

$$\bar{W}_R = A_2 \cos k_2\xi + B_2 \sin k_2\xi + C_2 \cosh k_2\xi + D_2 \sinh k_2\xi \qquad \xi_1 \leq \xi < 1 \qquad (2.32)$$

The constants A's and B's are obtained from the following eight boundary conditions :

Zero displacement at the ends gives

(i) at $\xi = 0$ $\quad \bar{W}_L = 0$ $\qquad$ 2.33(a)

(ii) at $\xi = 1$ $\quad \bar{W}_R = 0$ $\qquad$ 2.33(b)

Continuity of displacement, slope and bending moment at $\xi = \xi_1$ gives

(iii) at $\xi = \xi_1$ $\quad \bar{W}_L = \bar{W}_R$ 2.33(c)

(iv) at $\xi = \xi_1$ $\quad \bar{W}_L' = \bar{W}_R'$ 2.33(d)

(v) at $\xi = \xi_1$ $\quad \bar{W}_L'' = \bar{W}_R''$ 2.33(e)

non-dimensional bending moment (M1/EI) at end A is unity,

(vi) i.e. at $\xi = 0$ $\quad -\bar{W}_L''' + \frac{1}{2} \cdot \bar{k}_r \cdot \bar{W}_L' = 1$ 2.33(f)

where $\bar{k}_r = \frac{k_r l}{EI}$ is the non-dimensional rotational stiffness at the supports. Moment at end B is zero which gives

(vii) at $\xi = 1$ $\quad \bar{W}_R'' + \frac{1}{2} \cdot \bar{k}_r \cdot \bar{W}_R' = 0$ 2.33(g)

for the shear force balance at the mass

(viii) at $\xi = \xi_1$ $\quad -\bar{W}_L''' + \bar{W}_R''' = M_D/M_b \cdot \Omega_b^2 \cdot \bar{W}_{L/R}$ 2.33(h)

where $\Omega_b = \sqrt{\frac{M_b l^3}{EI}} \cdot \omega$ is the non-dimensional frequency of the beam, M_b is the mass of the beam ($= \rho Al$) and M_D is the mass of the disc.

The (8x8) matrix equation resulted from the above boundary conditions is given in Appendix-B. In the some way as described in Section 2.2, the receptances β_{AA}, β_{BB} and β_{AB} are evaluated from the constants A's and B's, C's and D's. Using these receptances, the complex propagation constant versus frequency (Ω_b) curve is obtained using Eqn. 2.9 and the plots are discussed in the next chapter.

CHAPTER 3

RESULTS AND DISCUSSIONS

3.1 Torsional Wave Propagation Characteristics

First of all let us consider an infinite periodic shaft shown in Fig. 3.1. The periodic element, AB, of this shaft is already shown in Fig. 2.4. Using the analysis presented in Chapter 2, the curve of torsional propagation constant $\mu_t (= \mu_{r,t} + i\mu_{i,t})$ versus the non-dimensional frequency, Ω_s, for this shaft is shown in Fig. 3.2. Both the real and imaginary parts of μ_t are shown in the same figure. The system under consideration being semi-definite, the first propagation zone starts from zero frequency as expected. Furthermore, there are alternate zones of propagation and attenuation. Figure 3.3 shows a similar plot for a different value of I_D/I_s with all other parameters being the same as in Fig. 3.2. With I_D equal to zero, i.e. for a homogeneous infinite shaft the same curve is as shown in Fig. 3.4. As is obvious all frequencies can propagate in an infinite homogeneous shaft with no periodic discontinuity. Equation C-1 in Appendix-C explains the nature of variation of $\mu_{i,t}$ with Ω_s and is depicted in Fig. 3.4. If one consider the other limiting case of $I_D/I_s \longrightarrow \infty$, i.e. the shaft inertia is neglected, then no propagation zone exists as the system becomes an infinite discrete system. The propagation constant curve only shows sudden jumps

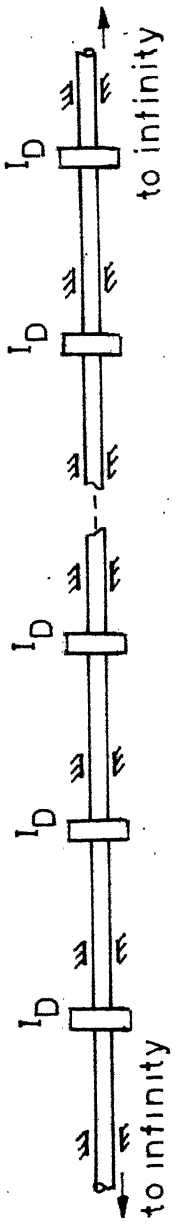

FIG. 3·1 INFINITE PERIODIC SHAFT

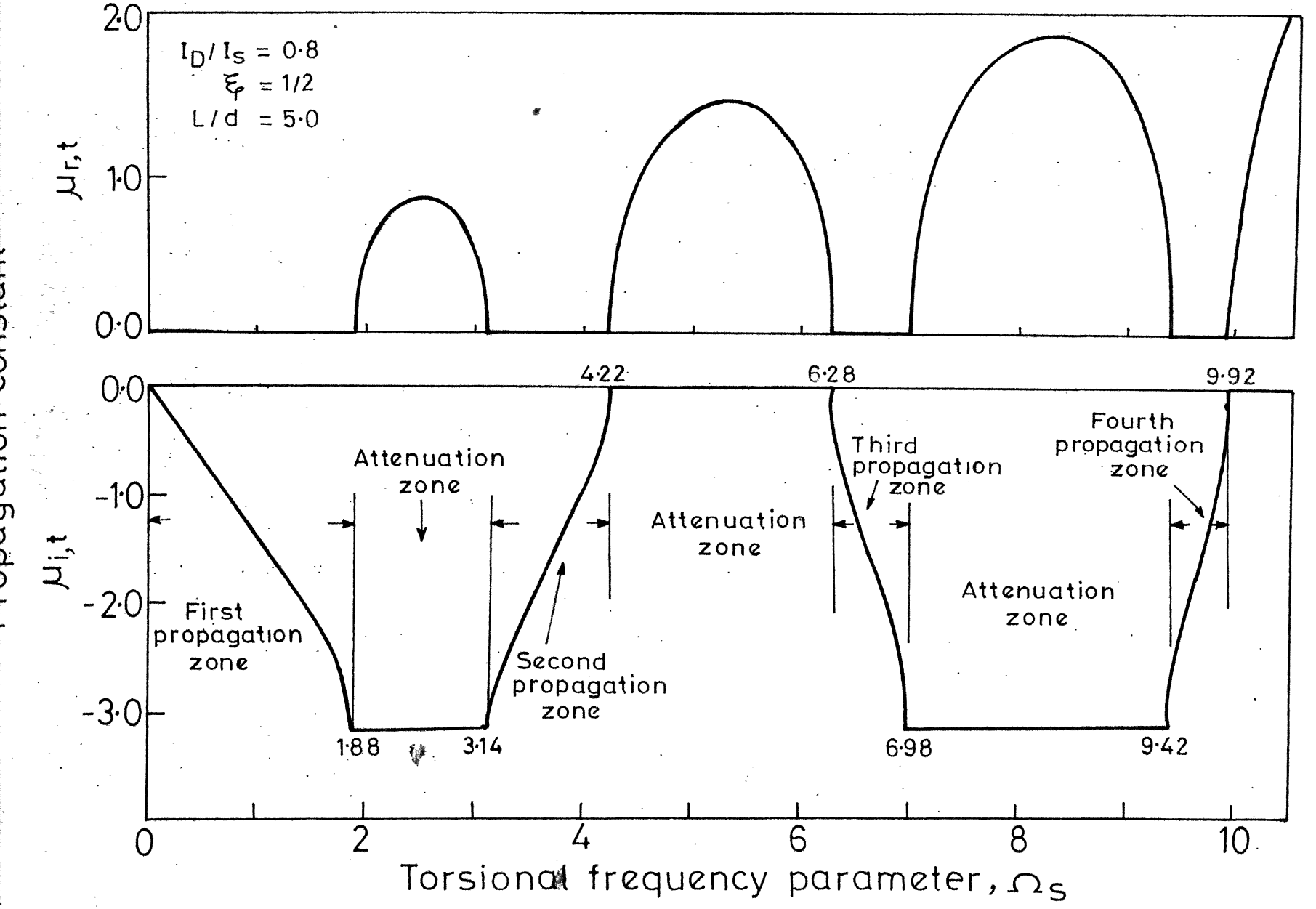

FIG. 3·3 VARIATION OF PROPAGATION CONSTANT WITH TORSIONAL FREQUENC

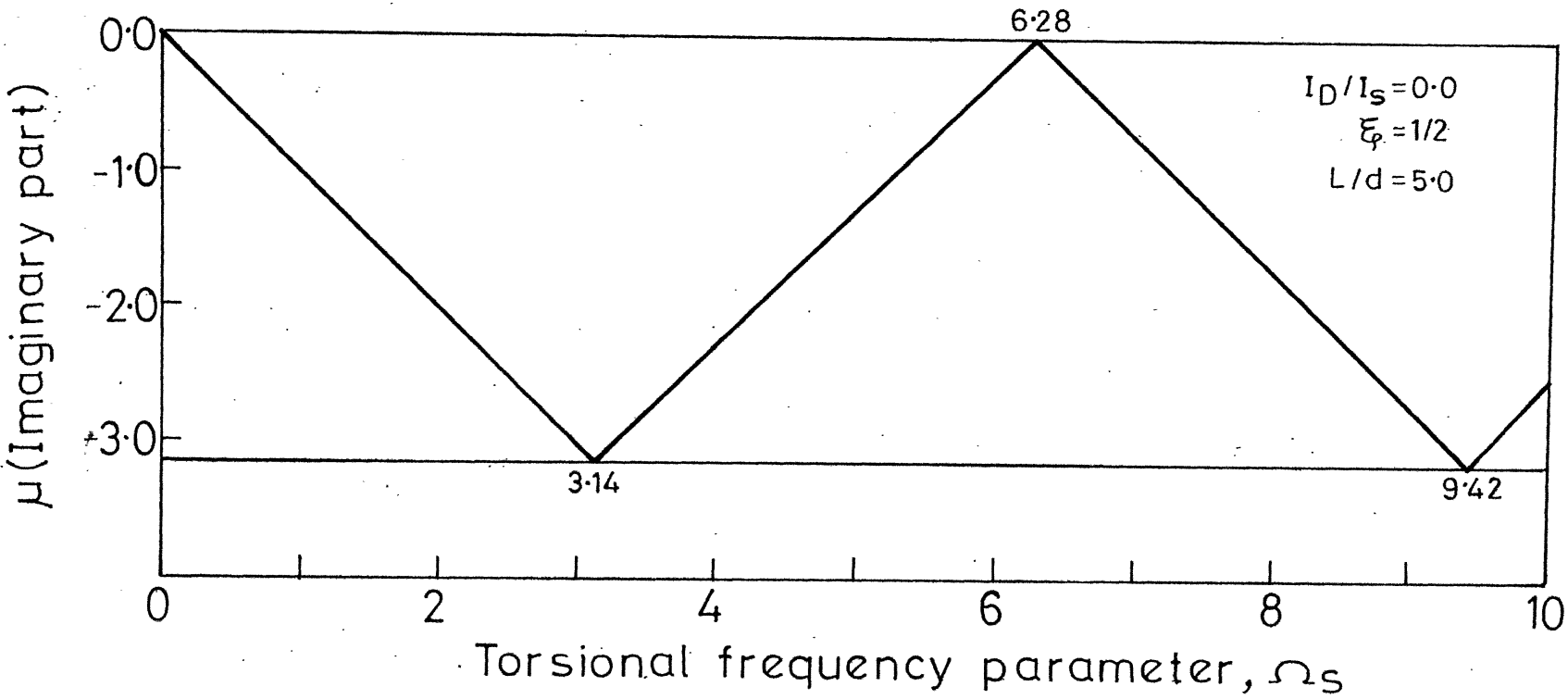

FIG·3·4 VARIATION OF PROPAGATION CONSTANT WITH TORSIONAL FREQUENCY

in values of $\mu_{i,t}$ from 0 to π and π to 0 whenever $\mu_{r,t} = 0$.

The curves of propagation constant versus frequency are independent of the variable ξ. Equation C-2 clearly shows μ_t to depend only on the frequency parameter, Ω_s, and the inertia ratio I_D/I_s. This result is also to be intuitively expected, because the bearings donot play any part so far as the torsional oscillations are concerned. So long the rotors are at a distance l apart, the propagation constant curves (Figs. 3.2 - 3.4) remain unchanged.

Figure 3.5 shows the band-widths of the first three attenuation zones for various values of the inertia ratio I_D/I_s. The band-widths are observed to increase with increase in inertia ratio but the rate of increase is more for $I_D/I_s \leq 1$ and it gradually flattens out for higher values of I_D/I_s. Table 3.1 shows the bounds of the first three propagation bands for various values of I_D/I_s. The N^{th} propagation band is seen to start from $\Omega_s = (N-1)\pi$. As obvious from the discussion presented earlier for the two limiting values of I_D/I_s, Table 3.1 also confirms that the propagation band-widths gradually diminish with increasing value of I_D/I_s.

3.2 Flexural Wave Propagation Characteristics

We now consider the results of flexural wave propagation constants (μ_b) for the infinite shaft shown in Fig.3.6. The periodic element of this structure is shown in Fig. 2.5. Figures 3.7 - 3.10 show the variation of μ_b with frequency for various parameters, namely, the mass ratio, M_D/M_b, the

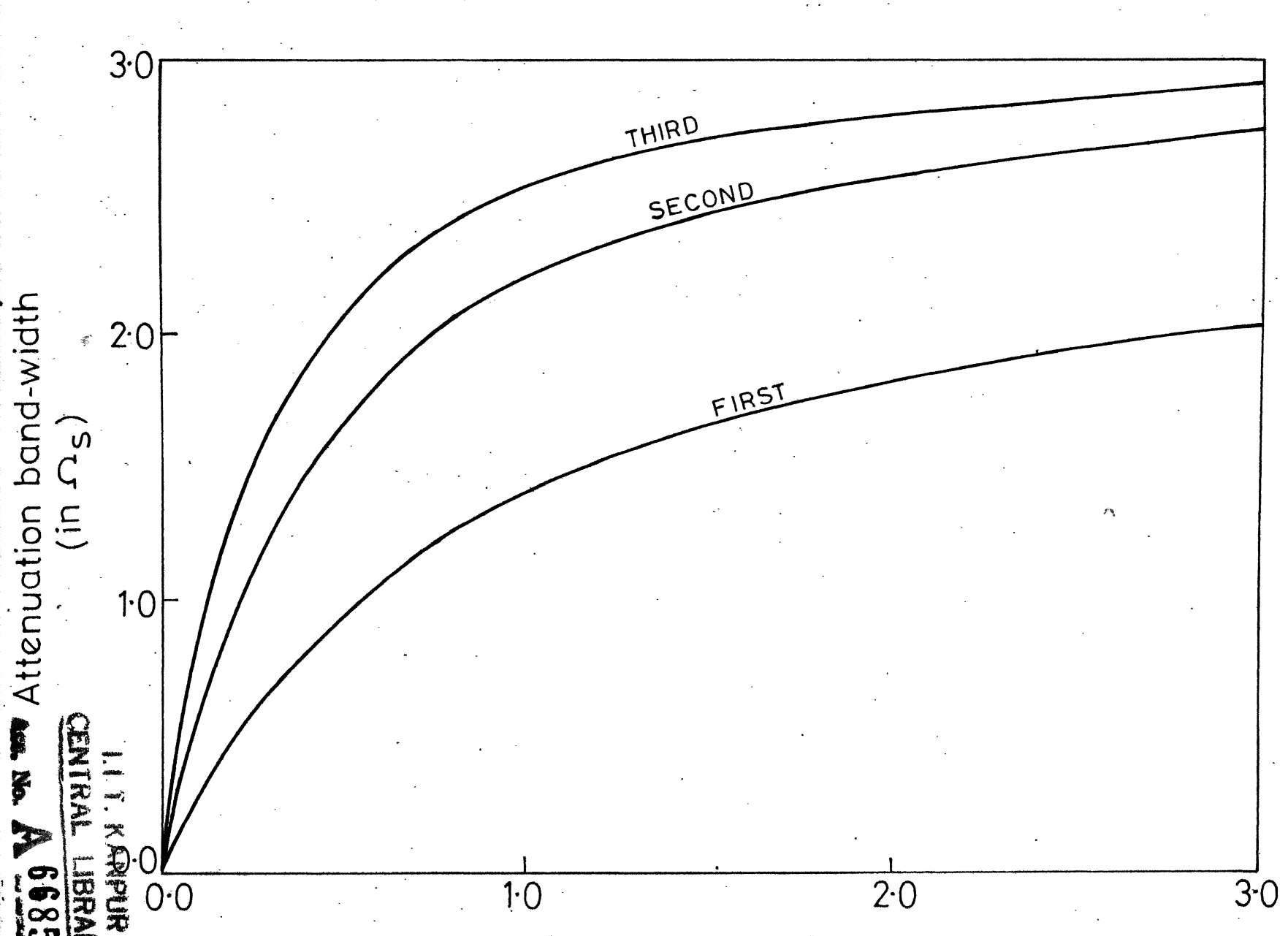

FIG.3·5 VARIATION OF ATTENUATION BAND-WIDTH WITH INERTIA RATIO

TABLE 3.1

BOUNDS OF PROPAGATION BANDS

I_D/I_s	Propagation Band		
	First	Second	Third
0.0	C O N T I N U O U S		
0.1	0.00 - 2.86 (2.86)*	3.14 - 5.74 (2.60)	6.28 - 8.61 (2.33)
0.2	0.00 - 2.64 (2.64)	3.14 - 5.32 (2.18)	6.28 - 8.08 (1.80)
0.8	0.00 - 1.88 (1.88)	3.14 - 4.22 (1.08)	6.28 - 6.98 (0.70)
1.2	0.00 - 1.62 (1.62)	3.14 - 3.96 (0.82)	6.28 - 6.78 (0.50)
2.0	0.00 - 1.32 (1.32)	3.14 - 3.68 (0.54)	6.28 - 6.60 (0.32)
3.0	0.00 - 1.10 (1.10)	3.14 - 3.52 (0.38)	6.28 - 6.50 (0.22)

*Quantities in brackets show the widths of the propagation bands.

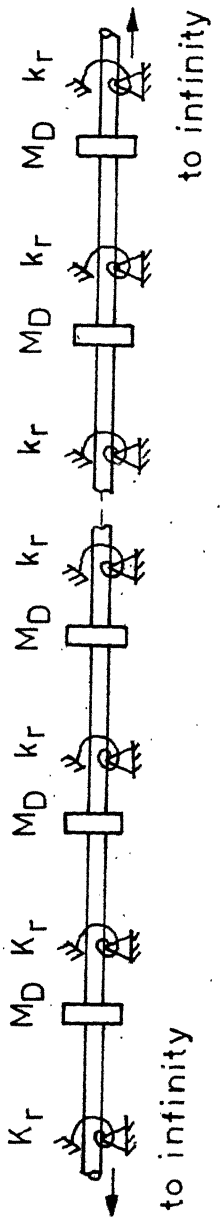

FIG. 3.6 INFINITE PERIODIC SHAFT IN FLEXURE

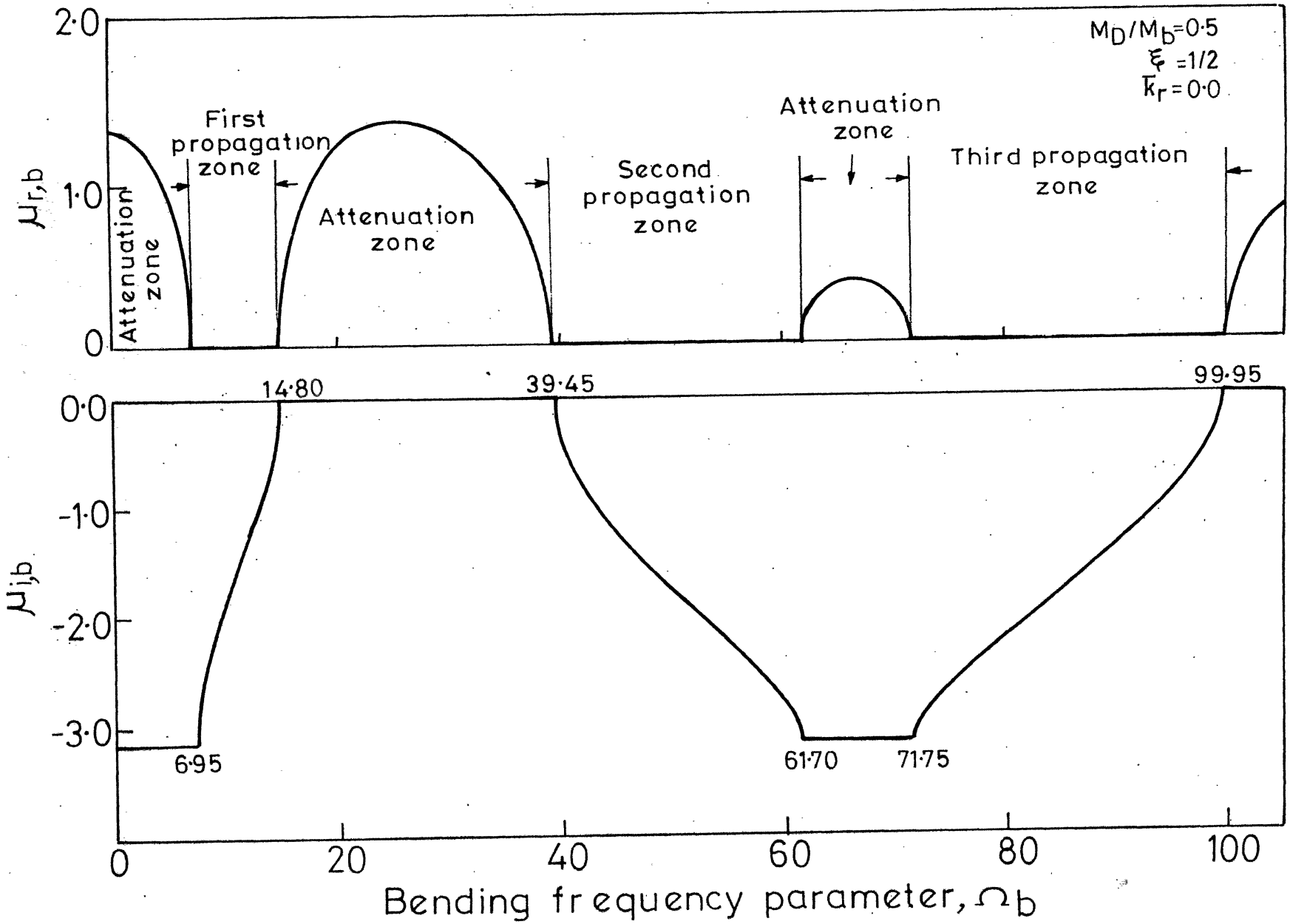

FIG.3·7 VARIATION OF PROPAGATION CONSTANT WITH BENDING FREQUENCY

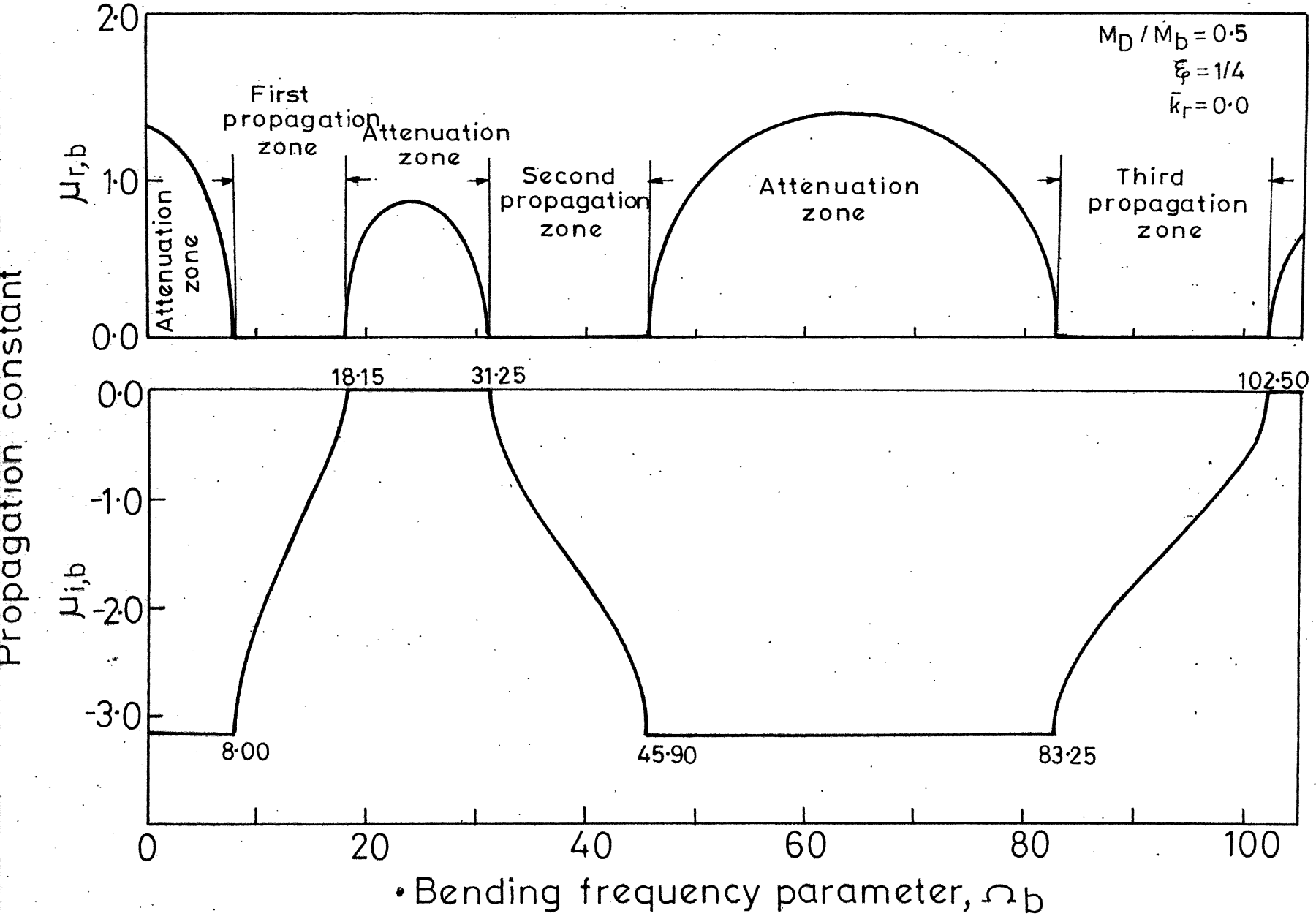

FIG·3·8 VARIATION OF PROPAGATION CONSTANT WITH BENDING FREQUENCY

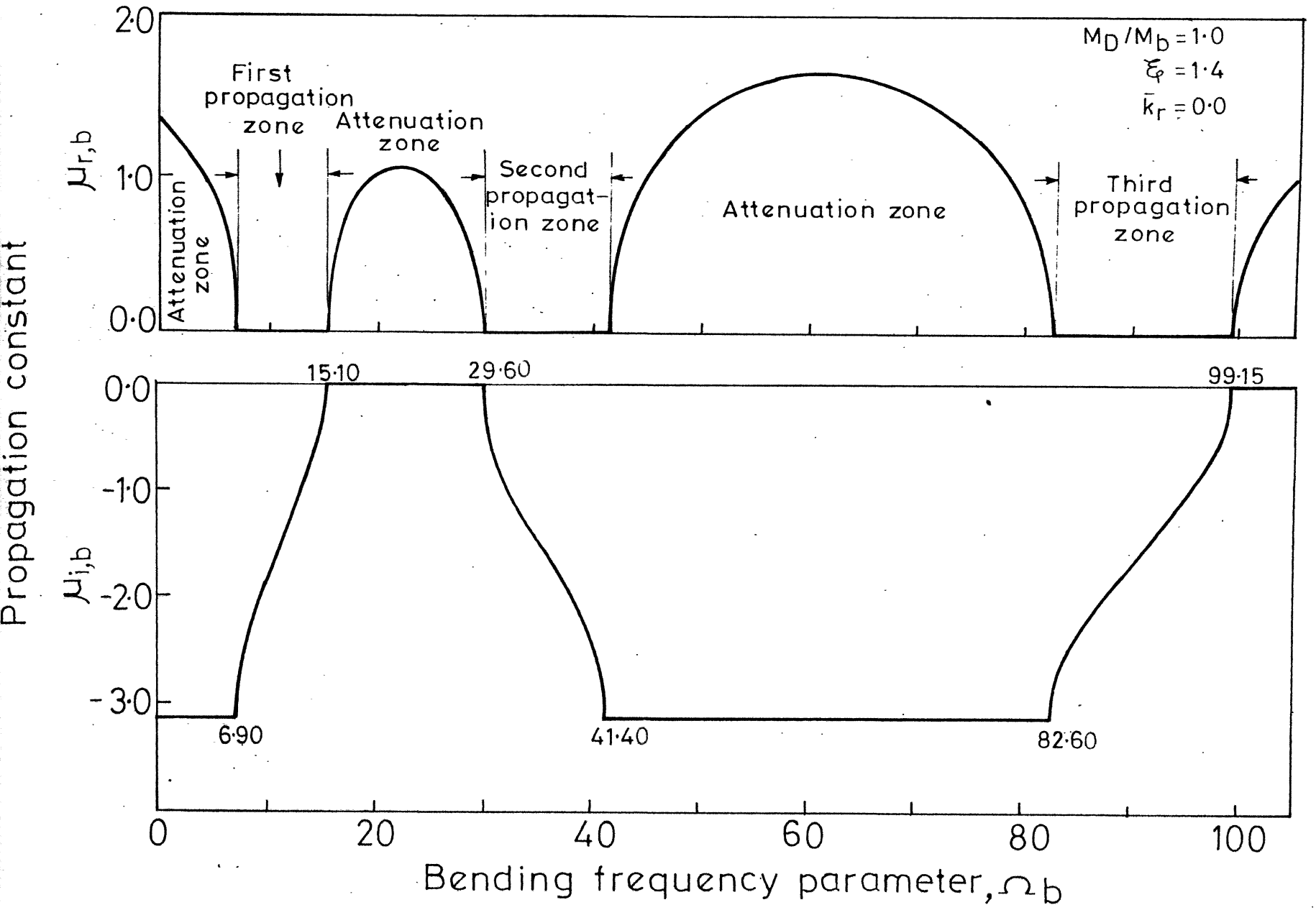

FIG.39 VARIATION OF PROPAGATION CONSTANT WITH BENDING FREQUENCY

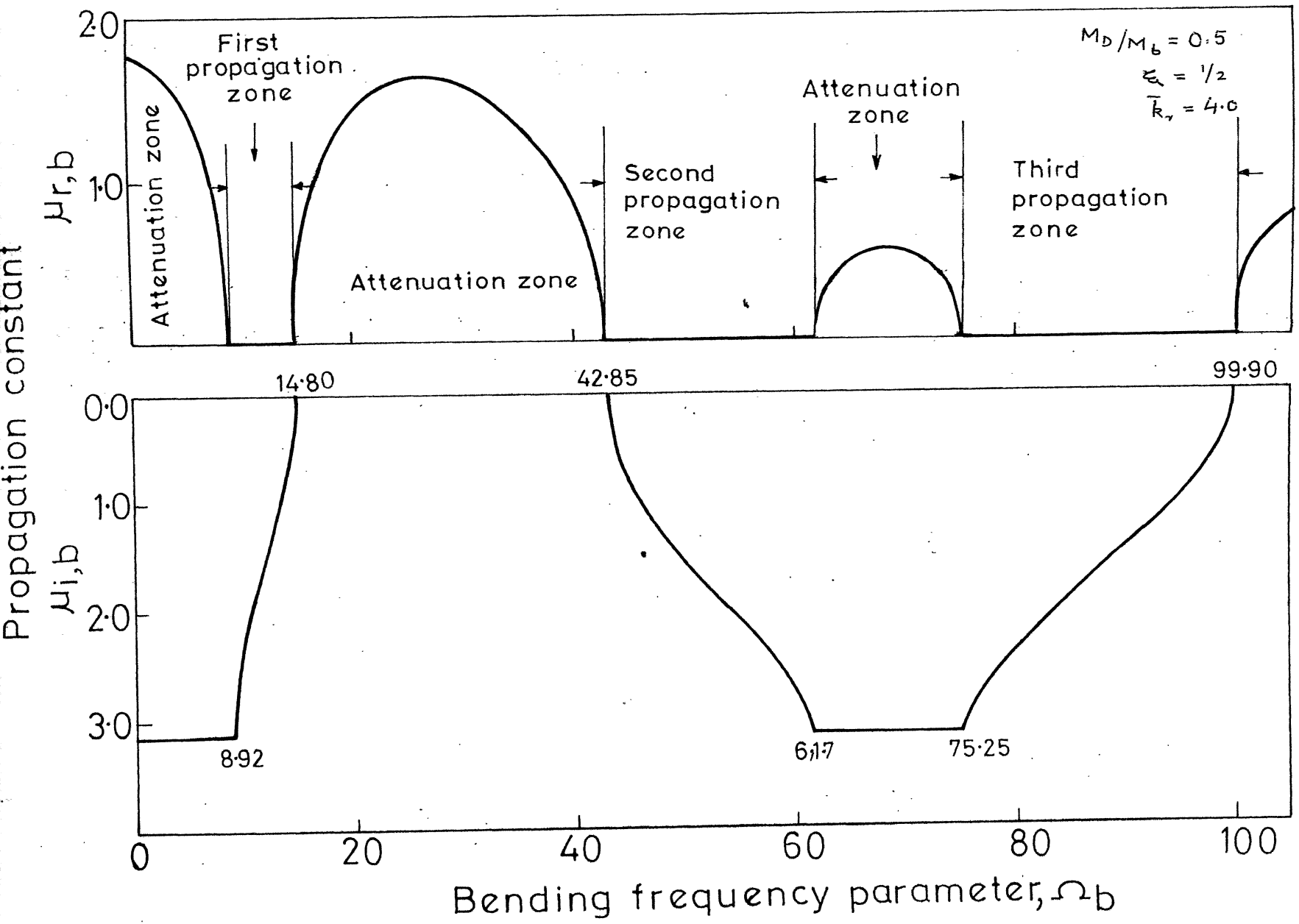

FIG. 3·10 VARIATION OF PROPAGATION CONSTANT WITH BENDING FREQUENCY

disc location parameter, ξ , and the non-dimensional rotational stiffness, $\bar{k}_r$. For flexural vibration, the system being positive-definite, the first frequency range is always an attenuation zone.

Comparing Figs. 3.7 and 3.8, it is seen that with increasing value of ξ (other parameters remaining same), both the bounds of the odd numbered propagation zones, i.e. first, third .... , shift to lower frequencies. Both the bounding frequencies of the even numbered propagation zones, however, shift to higher values. The difference in this behaviour in comparison to the torsional oscillation should be noted. This is because the bearings (consequently their locations) do affect the manner of flexural vibrations.

From the figures 3.8 and 3.9, it is observed that higher values of the mass ratio, M_D/M_b, depress both the bounding frequencies of every propagation band. The effect, in terms of percentage values, decreases with successive propagation bands. Comparison of Fig. 3.7 with Fig. 3.10 reveals that the rotational stiffness of the bearings increases only the lower bounding frequency of every propagation band where as the upper bounding frequencies remain unaffected. This is due to the fact that at the upper bounding frequency of every propagation band, the flexural wave mode has zero slope at the supports (Ref. 11).

Tables 3.2 and 3.3 show the bounds of the first three propagation bands for various values of the parameters. It is observed that for $\xi = 1/2$. the mass ratio parameter does not

TABLE 3.2

BOUNDS OF PROPAGATION BANDS IN FLEXURE

$\bar{k}_r = 0.0$

Propagation band	$\bar{\gamma}$	Disc to Shaft Mass Ratio, M_D/M_b				
		0.0	0.1	0.5	1.0	5.0
First	1/2	9.9 - 22.4 (12.5)*	9.0 - 20.0 (11.0)	7.0 - 14.8 (7.8)	5.7 - 11.9 (6.2)	3.0 - 6.0 (3.0)
	1/3	9.9 - 22.4 (12.5)	9.2 - 20.8 (11.6)	7.4 - 16.2 (8.8)	6.2 - 13.2 (7.0)	3.3 - 6.8 (3.5)
	1/4	9.9 - 22.4 (12.5)	9.4 - 21.6 (12.2)	8.0 - 18.2 (10.2)	6.9 - 15.1 (8.2)	3.9 - 8.0 (4.1)
Second	1/2	39.5 - 61.7 (22.2)	39.5 - 61.7 (22.2)	39.5 - 61.7 (22.2)	39.5 - 61.7 (22.2)	39.5 -61.7 (22.2)
	1/3	39.5 - 61.7 (22.2)	37.3 - 56.8 (19.5)	34.2 - 48.7 (14.5)	33.3 - 45.5 (12.2)	32.3 -41.4 (9.1)
	1/4	39.5 - 61.7 (22.2)	36.3 - 56.2 (19.9)	31.3 - 45.9 (14.6)	29.6 - 41.4 (11.8)	28.2 -35.6 (7.4)
Third	1/2	88.8 -121.0 (32.2)	82.1 -112.1 (30.0)	71.8 -100.0 (28.2)	67.9 - 95.7 (27.8)	63.2 -90.1 (26.9)
	1/3	88.8 -121.0 (32.2)	88.8 -120.1 (31.3)	88.8 -117.9 (29.1)	88.8 -116.5 (27.7)	88.8-114.7 (25.9)
	1/4	88.8 -121.0 (32.2)	86.0 -112.9 (26.9)	83.3 -102.5 (19.2)	82.6 - 99.2 (16.6)	81.9-95.5 (13.6)

*Quantitites in brackets show the widths of the propagation bands.

TABLE 3.3

BOUNDS OF PROPAGATION BANDS IN FLEXURE

$\bar{k}_r = 4.0$

Propagation band	$\zeta\eta$	Disc to Shaft Mass Ratio, M_D/M_b				
		0.0	0.1	0.5	1.0	5.0
First	1/2	12.8 – 22.4 (9.6)*	11.6 – 20.0 (8.4)	8.9 – 14.8 (5.9)	7.3 – 11.9 (4.6)	3.8 – 6.0 (2.2)
	1/3	12.8 – 22.4 (9.6)	11.9 – 20.8 (8.9)	9.6 – 16.2 (6.6)	8.0 – 13.2 (5.2)	4.3 – 6.0 (2.5)
	1/4	12.8 – 22.4 (9.6)	12.2 – 21.6 (9.4)	10.4 – 18.2 (7.8)	9.0 – 15.1 (6.1)	5.1 – 8.0 (2.9)
Second	1/2	42.9 – 61.7 (18.8)	42.9 – 61.7 (18.8)	42.9 – 61.7 (18.8)	42.9 – 61.7 (18.8)	42.9 – 61.7 (18.8)
	1/3	42.9 – 61.7 (18.8)	40.3 – 56.8 (16.5)	36.7 – 48.7 (12.0)	35.5 – 45.5 (10.0)	34.2 – 41.4 (7.2)
	1/4	42.9 – 61.7 (18.8)	39.3 – 56.2 (16.9)	33.5 – 45.9 (12.4)	31.4 – 41.4 (10.0)	29.5 – 35.6 (6.1)
Third	1/2	92.4 – 121.0 (28.6)	85.6 – 112.1 (26.5)	75.3 – 100.0 (24.7)	71.4 – 95.7 (24.3)	66.8 – 90.1 (23.3)
	1/3	92.4 – 121.0 (28.6)	92.4 – 120.1 (27.7)	92.4 – 117.9 (25.5)	92.4 – 116.5 (24.1)	92.4 – 114.7 (22.3)
	1/4	92.4 – 121.0 (28.6)	89.1 – 112.9 (23.8)	85.9 – 102.5 (16.6)	85.0 – 99.2 (14.2)	84.2 – 95.5 (11.3)

*Quantities in brackets indicate the widths of the propagation bands.

affect the bounds of the second band. This is because at these frequencies, the mid-point of every span is a nodal point. In fact, the same observation holds good for every even numbered propagation bands. For $\xi \neq 1/2$, all the propagation band-widths decrease with increasing mass ratio. For the same values of ξ and M_D/M_b, the propagation band-width increases for the successive bands.

Figures 3.11 and 3.12 show the variation of attenuation band-widths with the mass ratio for various values of ξ and $\bar{k}_r$. For symmetrical disc location ($\xi = 1/2$), the widths of odd numbered attenuation bands decrease with increase in mass ratio where as these of the even numbered band-widths increase. On the other hand, for unsymmetrical location of the disc, only first attenuation band-width is observed to decrease with increase in mass ratio and the third attenuation band-width shows an increasing trend. In this case, the second attenuation band-width shows an initial decrease but later increases at a slow rate with increase in mass ratio. However, in all the cases the attenuation band-widths do not change significantly beyond $M_D/M_b=1$.

3.3 Natural Frequencies of a Finite Shaft

Figure 3.13 shows an N span finite shaft which is loaded and supported periodically. The rotational stiffnesses at the end supports are taken as half of that at the intermediate bearings. This is done in order to maintain the periodicity of the overall structure. In this section, we discuss the the natural frequencies of the shaft both in bending and torsional modes. Figure 3.14 shows the variation of $\mu_{i,t}$ versus Ω_s. The same figure also contains the plots

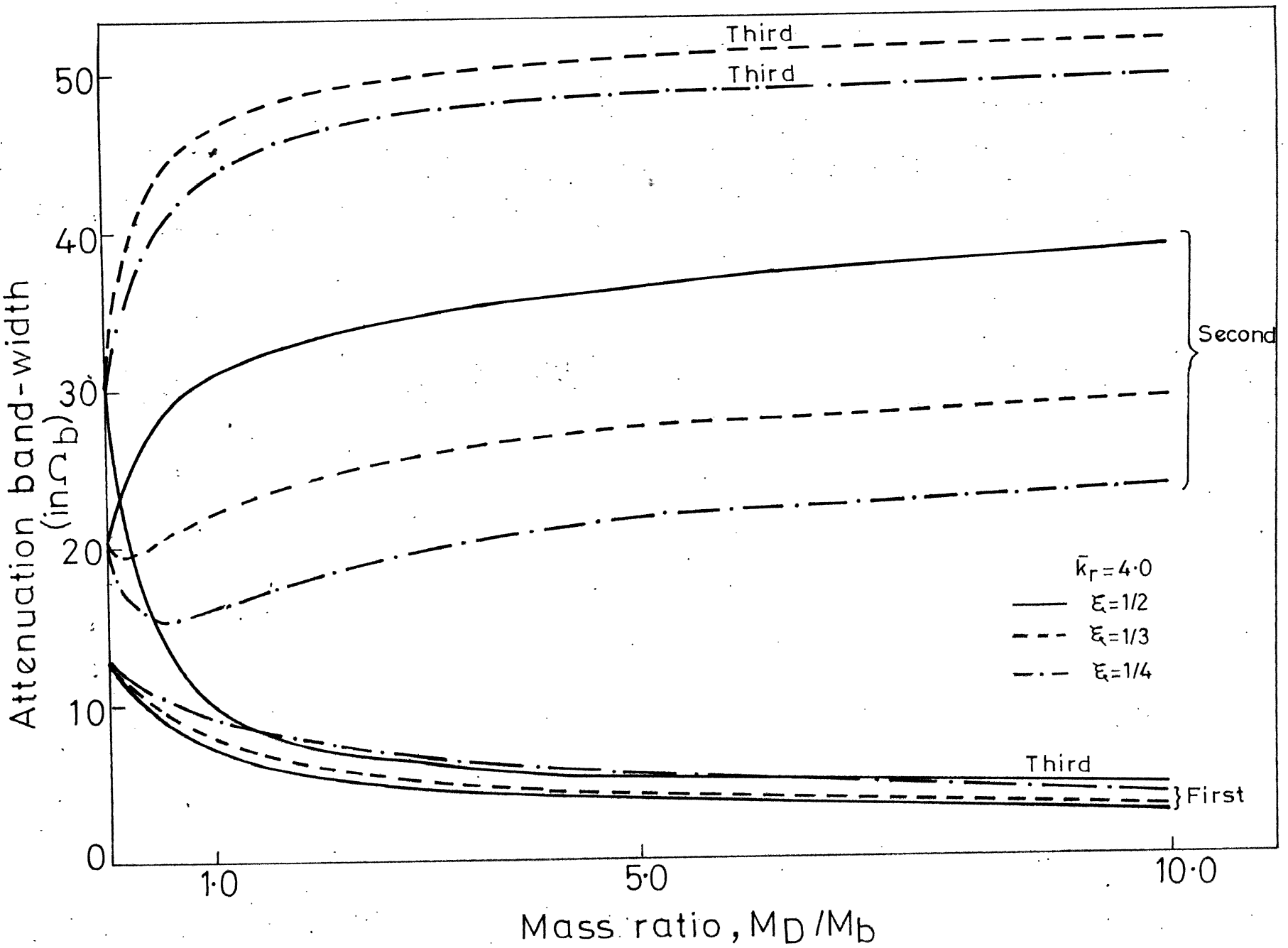

FIG.3·11 VARIATION OF ATTENUATION BAND-WIDTH WITH MASS RATIO

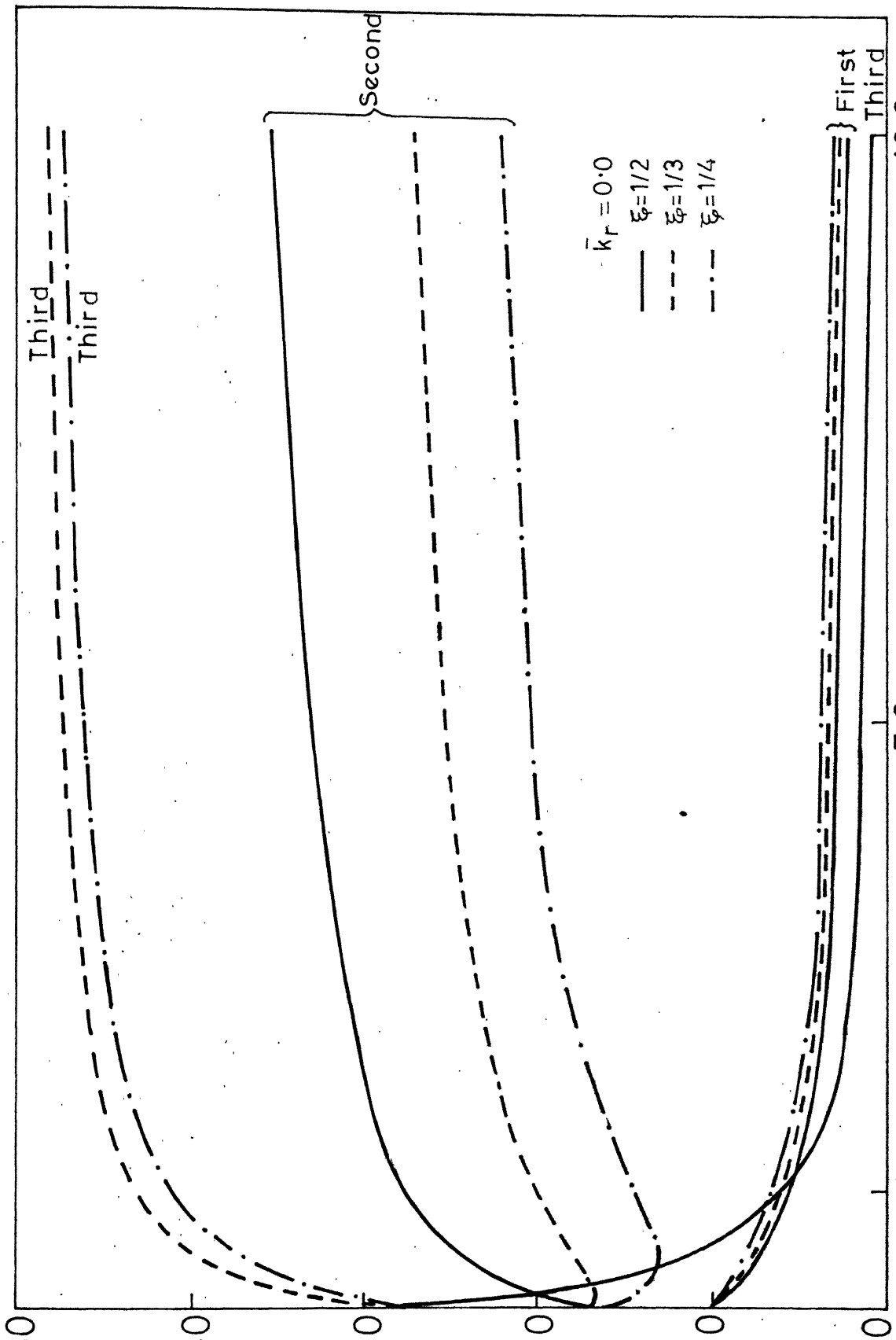

FIG.3·12 VARIATION OF ATTENUATION BAND WIDTH WITH MASS RATIO

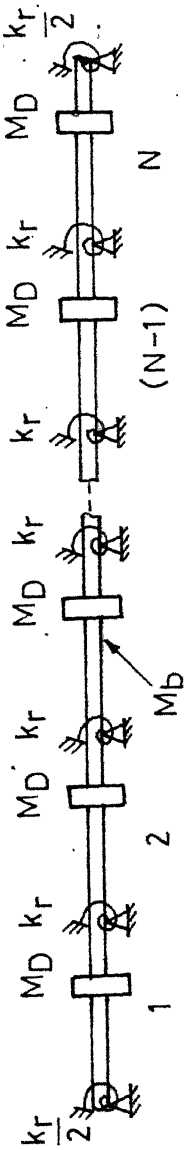

FIG·3·13 N-SPAN FINITE SHAFT IN FLEXURE

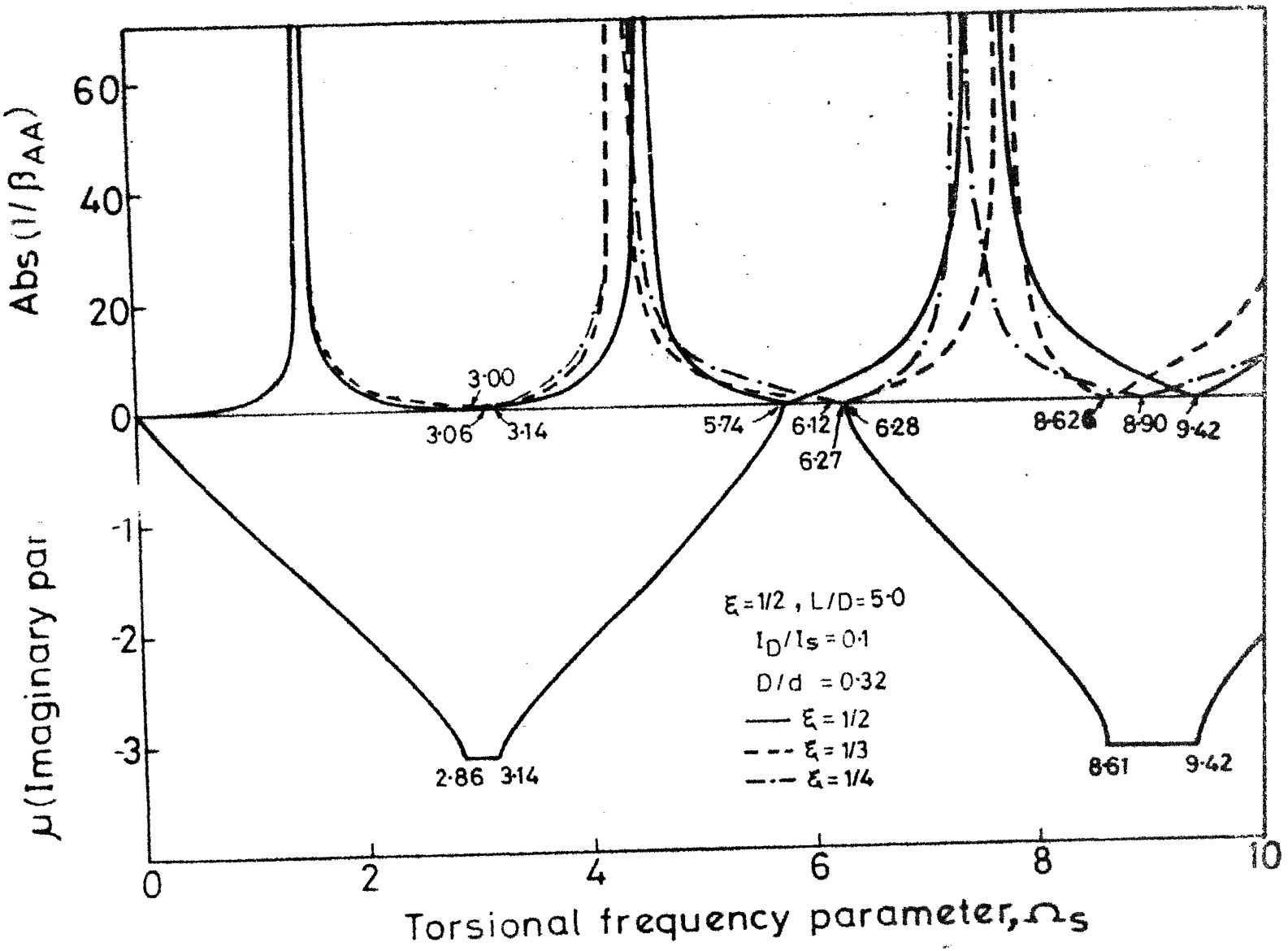

FIG.3·14 LOCATION OF NATURAL FREQUENCIES(TORSIONAL) IN ATTENUATION BANDS

of Abs $(1/\beta_{AA})$ in torsion, for various values of ξ.

As discussed in Chapter 2, in general, every propagation zone contains (N-1) natural frequencies and every N^{th} natural frequency is given by Abs $(1/\beta_{AA}) = 0$. Thus, out of every N natural frequencies, only one frequency depends on the value of ξ. These particular natural frequencies depending on ξ are nothing but the natural frequencies of the periodic element shown in Fig. 2.4. For symmetric location of the disc, i.e., $\xi = 1/2$, Abs $(1/\beta_{AA})$ goes to zero at the bounding frequencies of the propagation bands. Hence, in this case all the natural frequencies can be considered to lie in the propagation bands. The natural frequencies lying in the propagation bands can be easily determined by the graphical procedure explained in Fig. 2.3. These are the values of Ω_s corresponding to $\mu_{i,t} = m\pi/N$, m varying from 1, 2,....(N-1). The natural frequencies lying in the first three attenuation bands are tabulated in Table 3.4.

Figure 3.15 and 3.16 show the results for the flexural oscillation for two different values of ξ. Again for $\xi = 1/2$, it is seen that all the natural frequencies are contained within the propagation zones. For $\xi \neq 1/2$, one out of every N natural frequencies lies in the attenuation bands corresponding to Abs $(1/\beta_{AA}) = 0$ in bending. Unlike in the case of torsional oscillation, in this case the natural frequencies lying within propagation bands, also depend on the value of ξ. This is due to the dependence of the propagation constant itself on the value of ξ. In every case, the natural

TABLE 3.4

N^{th} TORSIONAL NATURAL FREQUENCY FOR VARIOUS I_D/I_s AND ξ

ξ	I_D/I_s	Attenuation bands		
		First	Second	Third
1/2	0.1	3.14	5.74	9.42
	0.2	3.14	5.32	9.42
	0.8	3.14	4.22	9.42
1/3	0.1	3.06	6.12	8.626
	0.2	3.00	5.96	8.14
	0.8	2.76	5.34	7.36
1/4	0.1	3.00	6.27	8.90
	0.2	2.90	6.27	8.40
	0.8	2.56	6.27	7.16

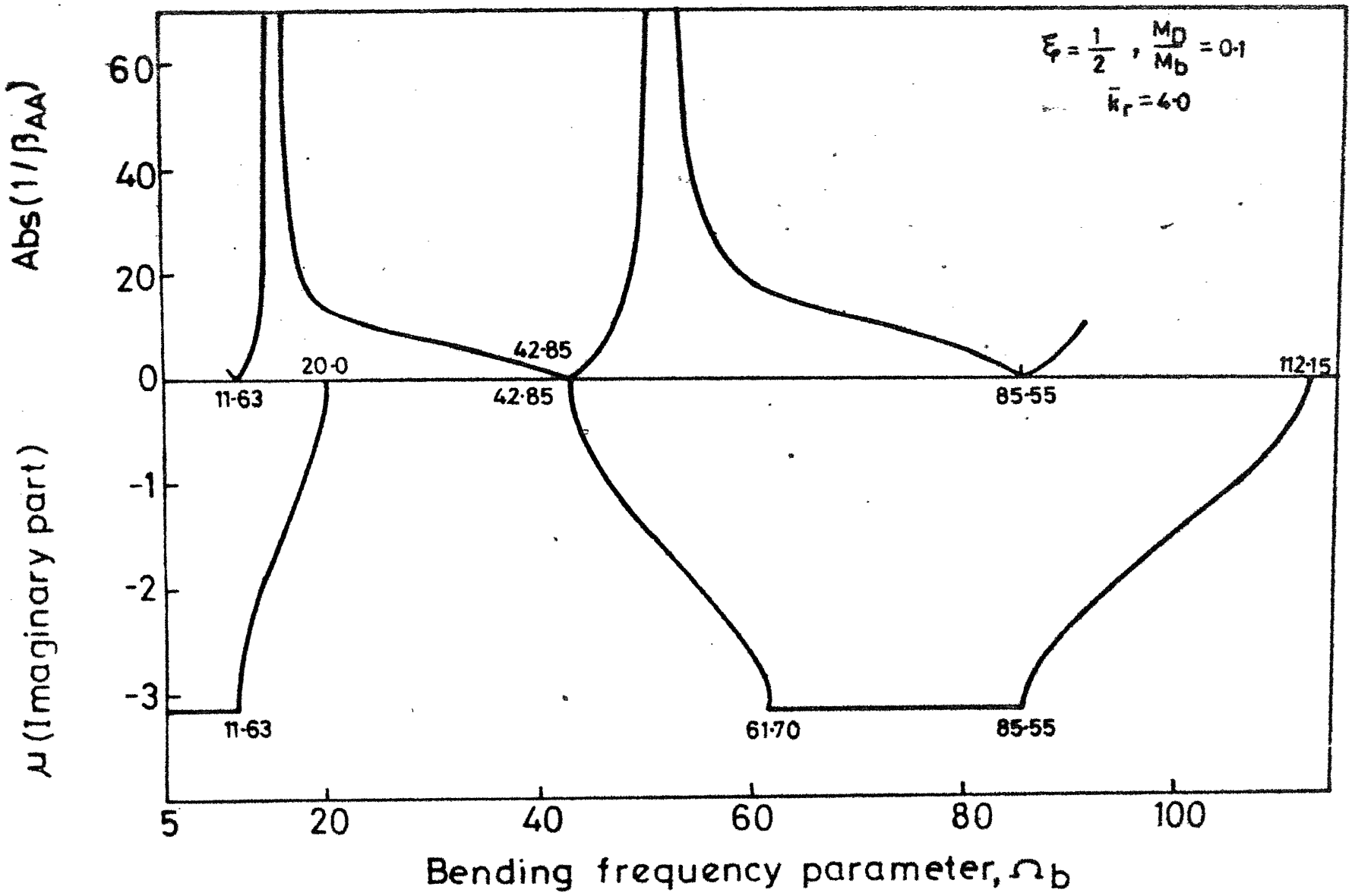

FIG.3·15 LOCATION OF NATURAL FREQUENCIES (BENDING) IN ATTENUATION BANDS

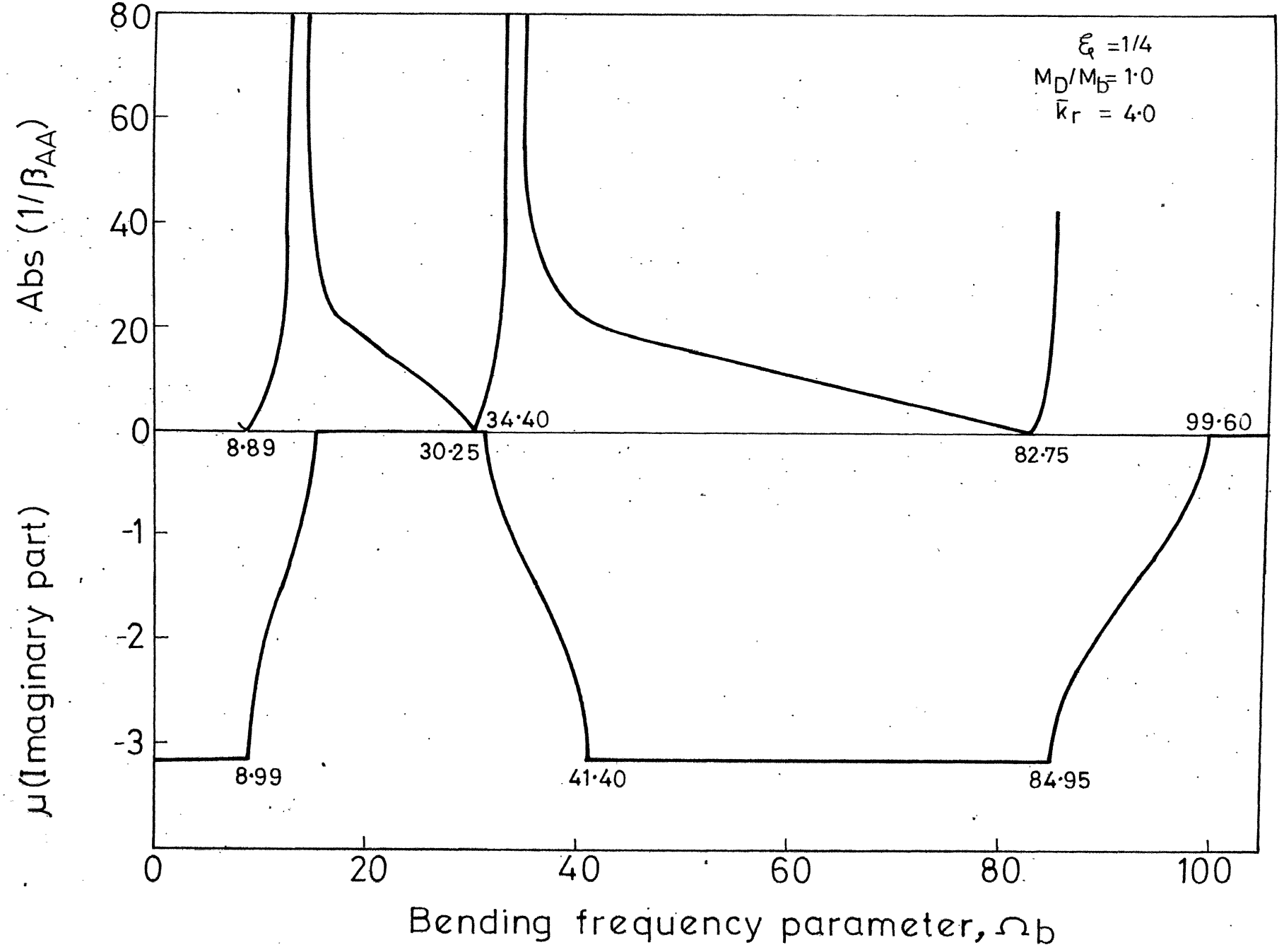

FIG.3·16 LOCATION OF NATURAL FREQUENCIES (BENDING) IN ATTENUATION BANDS

frequencies lying within the propagation bands are again determined by the graphical procedure. Table 3.5 gives the natural frequencies lying in the first three attenuation bands for various values of the parameters involved.

3.4 Frequency Range of Operation

We have already seen that most of the natural frequencies of an N span shaft lie within the propagation bands of the corresponding infinite shaft. In fact, for symmetrical location of the disc between the adjacent bearings, all the natural frequencies lie within the propagation bands. Hence if the torsional and the bending propagation bands are overlapped by proper choice of parameters, a speed range of operation can be found which is free from both torsional and flexural resonances. This possibility is explored in this section by attempting to match the propagation bands as far as possible. In this connection the first torsional propagation band starting from zero frequency is not taken into consideration. The M^{th} bending propagation band is attempted to be matched with the $(M+1)^{th}$ torsional propagation band. In the discussion to follow, symmetrically placed rotors ($\xi = 1/2$) are assumed to be discs of diameter D so that $I_D = M_D.D^2/8$.

The bending propagation bands are always found to be much wider than those in torsion. So as a compromise, instead of good matching of the two types of propagation bands, an attempt is made to contain the entire torsional propagation band within the bending propagation band. It can easily be shown

TABLE 3.5

N^{th} BENDING NATURAL FREQUENCY FOR VARIOUS M_D/M_b AND ξ

$\bar{k}_r = 4.0$

ξ	M_D/M_b	Attenuation bands		
		First	Second	Third
1/2	0.0	12.79	42.85	92.40
	0.1	11.63	42.85	85.55
	0.5	8.925	42.85	75.25
	1.0	7.2466	42.85	71.40
1/3	0.0	12.79	42.85	92.40
	0.1	11.913	40.20	92.3945
	0.5	9.560	35.80	92.378
	1.0	7.92	33.95	92.370
1/4	0.0	12.79	42.85	92.40
	0.1	12.209	39.325	88.80
	0.5	10.384	32.95	84.20
	1.0	8.89	30.25	82.75

that for a material with Poisson's ratio $\nu = 0.3$, Ω_b and Ω_s are related as follows :

$$\Omega_b = \Omega_s \cdot \frac{4}{\sqrt{2.6}} \cdot L/d \qquad (3.1)$$

Keeping in mind that the $(M+1)^{th}$ torsional propagation band always starts at $\Omega_s = M\pi$ and lies within the range $M\pi \leq \Omega_s \leq (M+1)\pi$, if one attempts to match the start of this band with that of the M^{th} bending propagation band, the resulting values of both L/d and D/d are rather low. Much more realistic values of these parameters are obtained if one attempts, instead, to match the end of these bands. In figures 3.17 and 3.18 both the torsional and the bending propagation bands are plotted against the common abscissa Ω_b, i.e. the bending frequency parameter. These two figures refer to two different values of the mass ratio parameter M_D/M_b. In figures 3.17 (a), (b) and (c) two torsional propagation bands are indicated for two different sets of values of L/d and D/d. The first set of these values matches the start of the M^{th} bending band with that of the $(M+1)^{th}$ torsional band, where-as the other matches the ends of these bands. The first set of values obtained from Fig. 3.17 are also included in Table 3.6. It is evident that the values of L/d and D/d are not acceptable from practical considerations. In Fig. 3.18 only the ends of the bending and the torsional propagation bands are matched.

With a fixed value of D/d = 3.5, the best possible matching obtained in various cases are reported in Table 3.7. In each

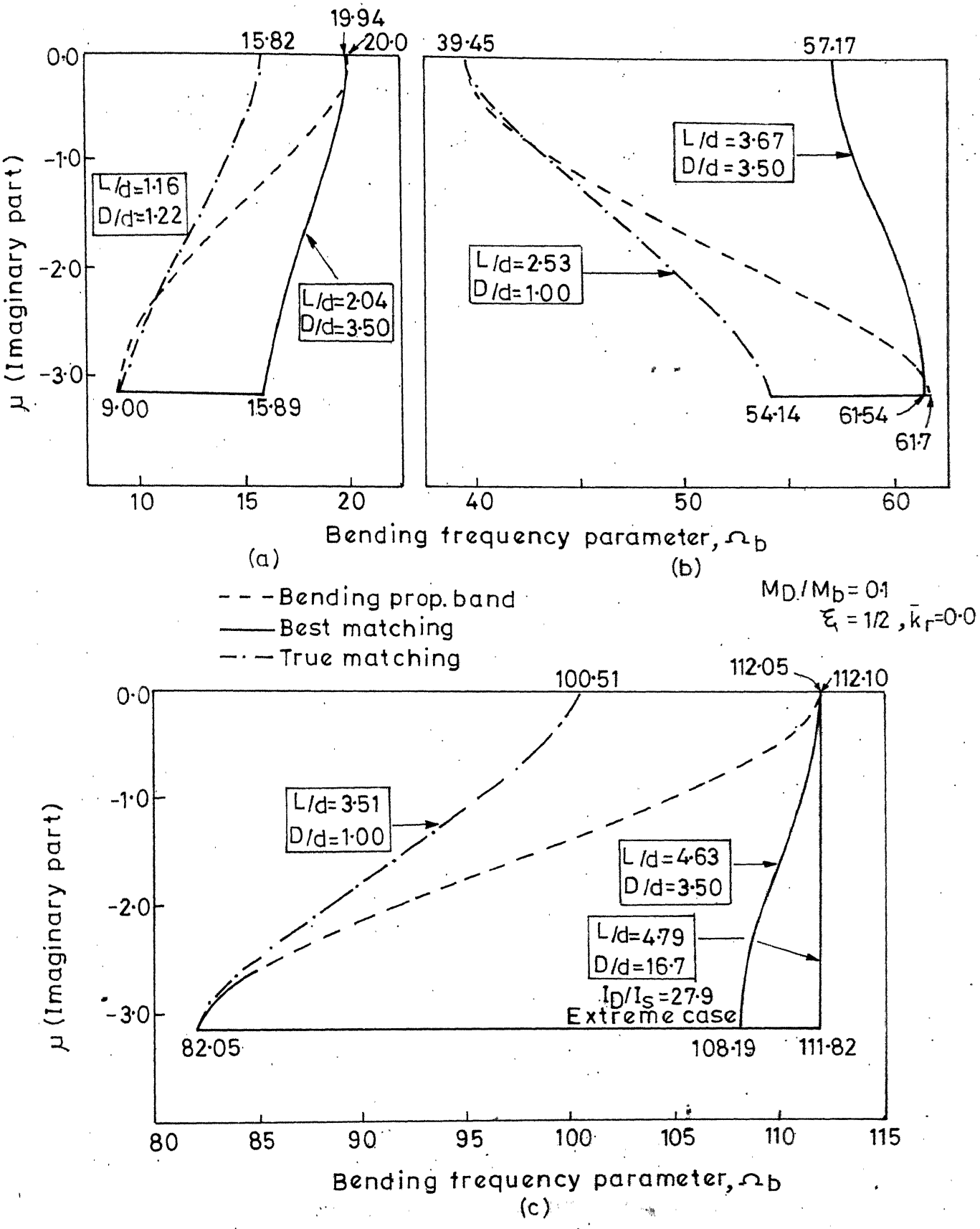

FIG. 3·17 MATCHING OF BENDING AND PROPAGATION BANDS

(a) M=1; (b) M=2; and (c) M=3

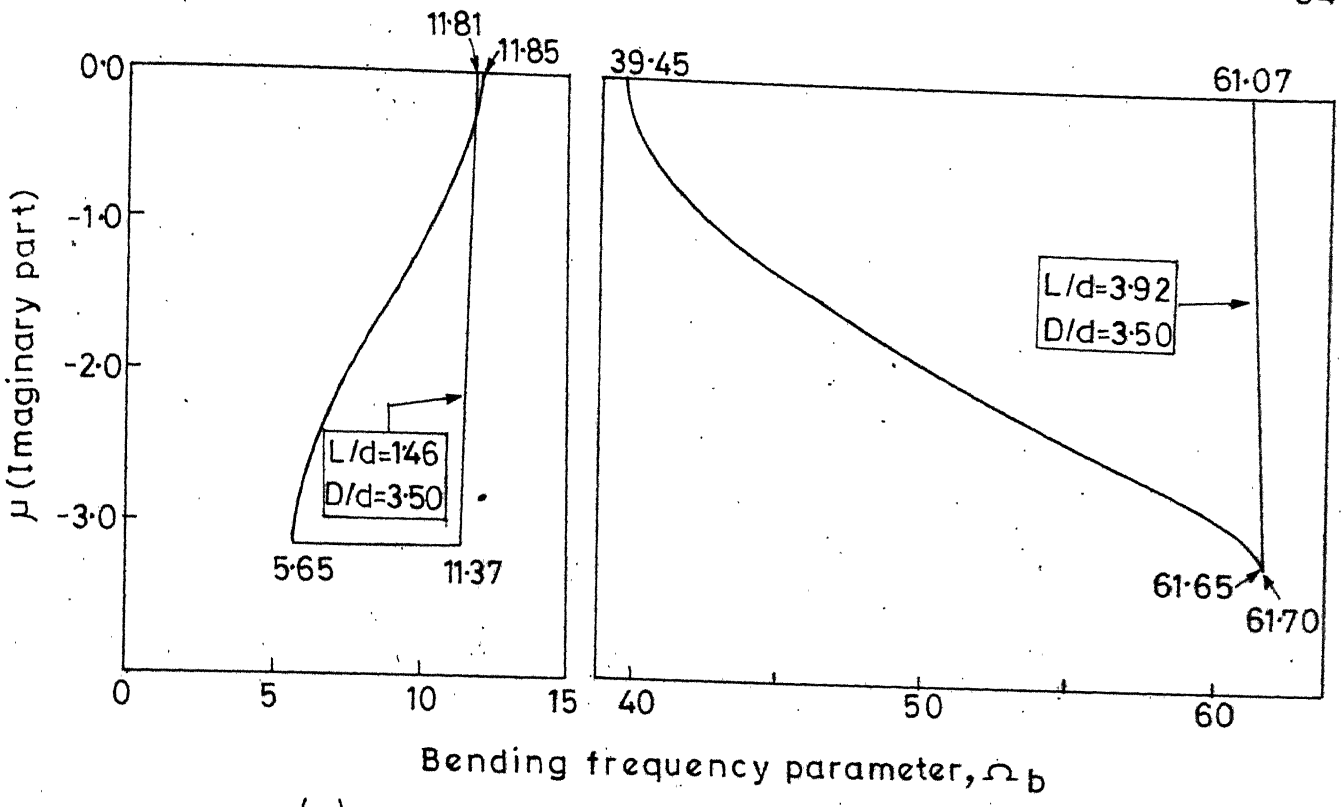

$M_D / M_b = 1·0$

$\xi = 1/2$

$k_r = 0·0$

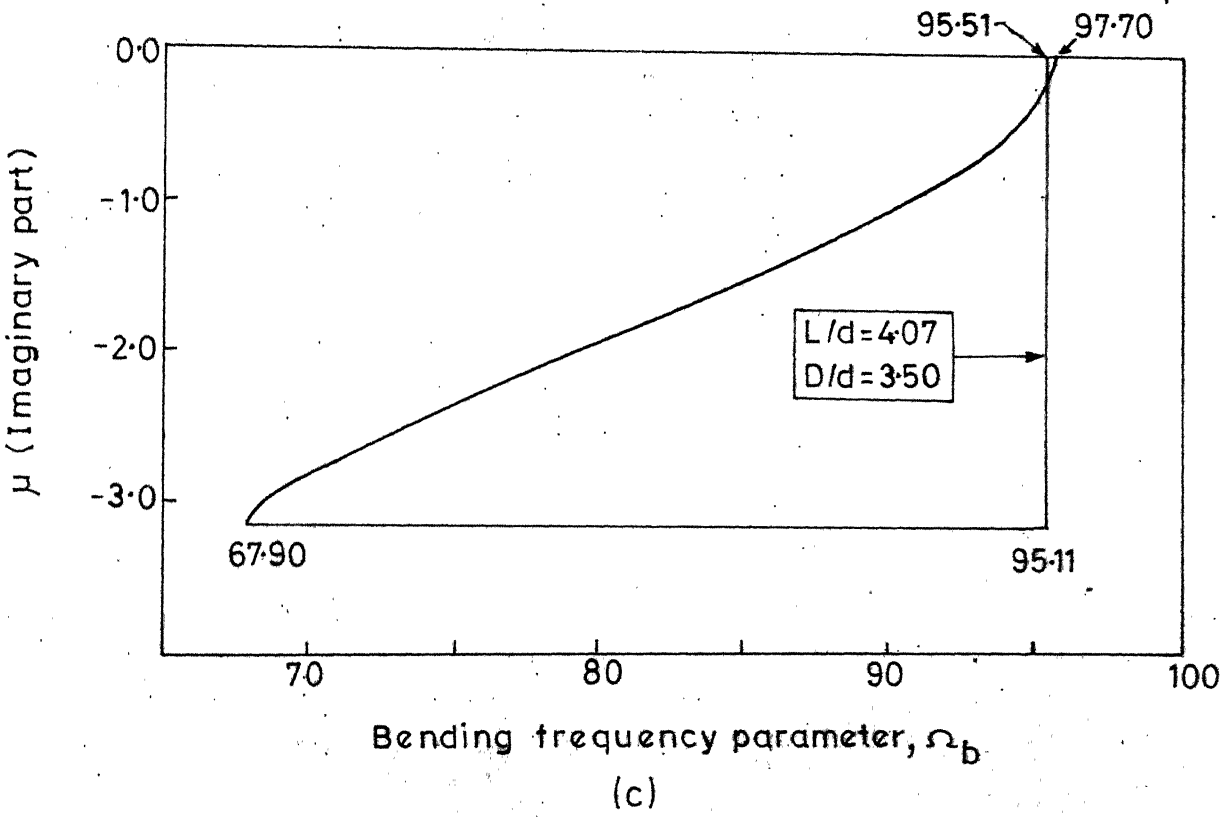

FIG. 3·18 MATCHING OF BENDING AND TORSIONAL PROPAGATION BANDS (a) M=1 (b) M=2 and (c) M=3

TABLE 3.6

PROPAGATION BANDS IN FLEXURE AND TORSION

$M_D/M_b = 0.1, \qquad \xi = 1/2, \qquad \bar{k}_r = 0.0$

Propagation band	End frequencies in bending (in Ω_b)	End frequencies in torsion (in Ω_b)	L/d ratio	D/d ratio
First	9.00 - 20.00	8.997 - 15.816	1.155	1.22
Second	39.45 - 61.70	39.445 - 54.143	2.532	1.00
Third	82.05 -112.10	82.046 -100.510	3.511	1.00

TABLE 3.7

PROPAGATION BANDS IN FLEXURE AND TORSION

$\xi = 1/2, \qquad \bar{k}_r = 0.0$

M_D/M_b	Propagation band	End frequencies in flexure (in Ω_b)	Best matching end frequencies in torsion (in Ω_b)	L/d ratio	D/d ratio
0.1	First	9.00 - 20.00	15.890 - 19.939	2.04	3.5
	Second	39.45 - 61.70	57.174 - 61.544	3.67	3.5
	Third	82.05 -112.10	108.194 -112.100	4.63	3.5
0.5	First	6.95 - 14.80	13.865 - 14.748	1.78	3.5
	Second	39.45 - 61.70	60.446 - 61.601	3.88	3.5
	Third	71.75 - 99.95	99.081 - 99.922	4.24	3.5
1.0	First	5.65 - 11.85	11.372 - 11.807	1.46	3.5
	Second	39.45 - 61.70	61.069 - 61.652	3.92	3.5
	Third	67.90 - 95.70	95.108 - 95.512	4.07	3.5

case, it is seen that the entire torsional band is contained within the corresponding flexural band. Thus the entire attenuation bands for flexural oscillations are free from both torsional and bending resonances.

It is already seen in section 3.2, that the start of every flexural propagation band can be shifted to higher frequencies without affecting its upper bounding frequency by providing rotational stiffness at the supports. In other words, the flexural attenuation band-widths can be widened in this manner. From the results presented in Table 3.7, it may be noted that there is enough provision for shifting the start of the bending propagation bands to higher frequencies without interfering with the torsional bands. Hence, upon introduction of rotational stiffnesses, $\bar{k}_r$, at the supports, a still wider range of operational speed for the shaft can be obtained without causing any kind of resonance.

3.5 Effect of Bearing Flexibility in Transverse Direction

From the discussion presented in previous sections, it is seen that in the context of wider operating speed range of the shaft, it is better to reduce the propagation band-widths in flexural oscillations. To this end, we consider an infinite shaft loaded and supported periodically as shown in Fig. 3.19. The only difference in this case with that considered earlier, is the presence of bearing flexibility, k_t. The stiffness of the bearing in transverse direction, k_t, is non-dimensionalised as

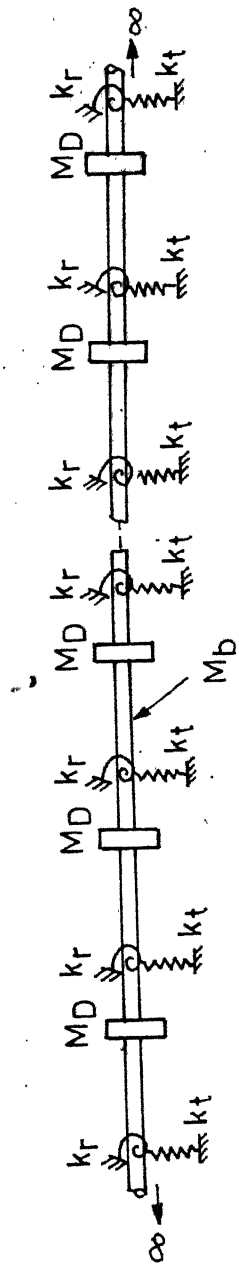

FIG. 3·19 INFINITE PERIODIC SHAFT IN FLEXURE WITH ROTATIONAL AND TRANSVERSE STIFFNESS AT THE SUPPORTS

$$\bar{k}_t = k_t l^3/EI \qquad (3.2)$$

With the introduction of k_t, the system becomes a bi-coupled periodic system wherein two pairs of propagation constants are involved [14]. These propagation constants can be determined by the same receptance method outlined in Chapter 2, after modifying the necessary boundary conditions and the equation for the propagation constant. The mathematical analysis for this purpose is included in Appendix-D.

The propagation constant curve for a typical case is shown in Fig. 3.20. Comparing the first propagation band in this figure with the result given in Table 3.3 for the similar case with $k_t \rightarrow \infty$, the following observation can be made.

With the introduction of the bearing flexibility in transverse direction, the start of the band remains unaffected, whereas the end of the band is shifted to lower frequency. In other words, the first propagation band is narrowed down considerably. Thus, it may be worthwhile to explore the effectiveness of bearing flexibility in widening the operating speed range of the shaft.

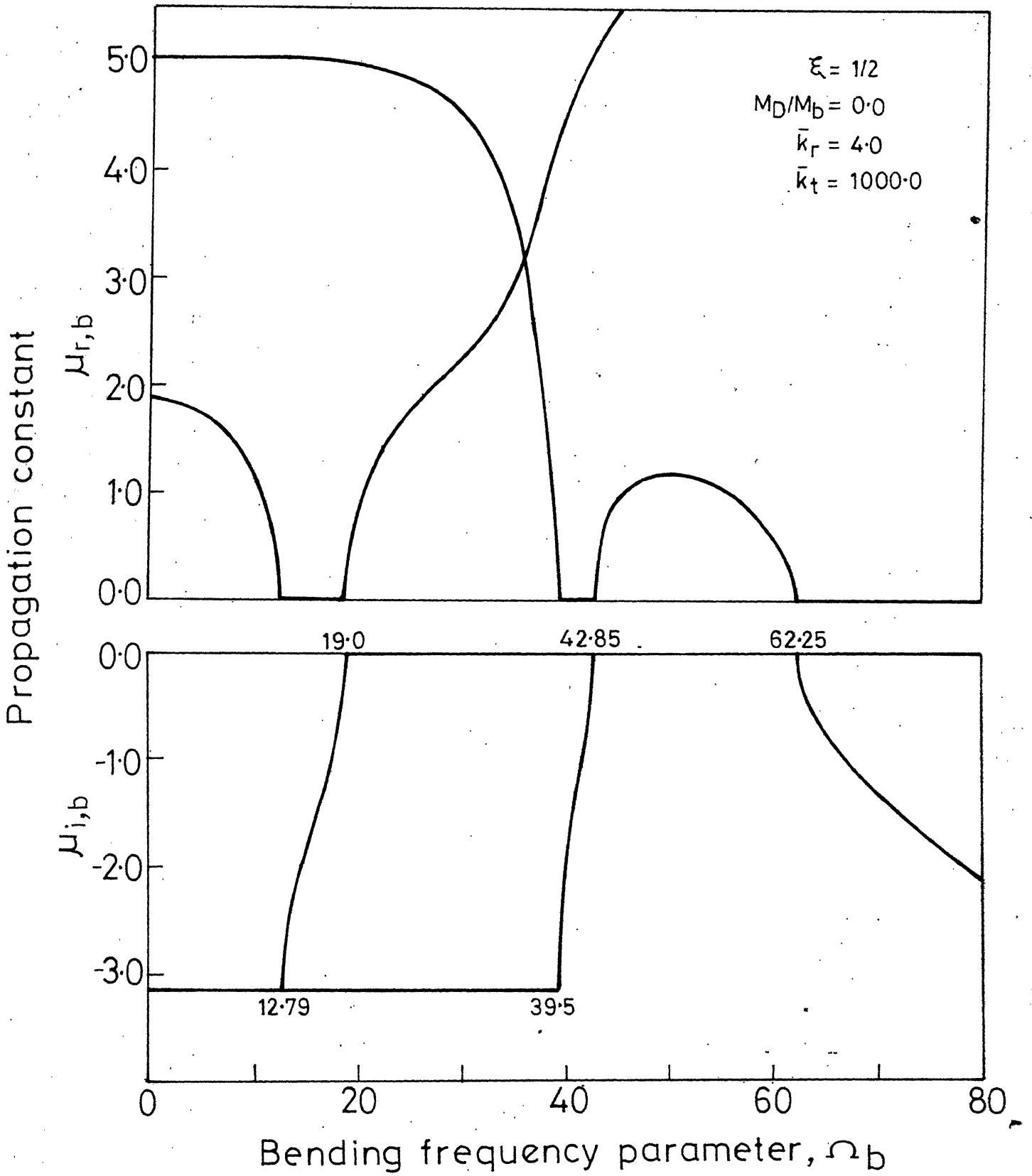

FIG. 3·20 BENDING PROPAGATION CONSTANTS FOR SHAFT WITH FLEXIBLE SUPPORTS

CHAPTER 4

CONCLUSIONS

On the basis of the results presented in the thesis, several important conclusions can be made, They are listed below :

(i) The wave approach is most suitable for determining the bending and the torsional natural frequencies of a shaft which is loaded and supported periodically. Unlike in other methods, here the computational effort remains independent of the number of spans.

(ii) For an N span periodic shaft, (N-1) torsional natural frequencies out of every N remain unaffected by the location of the lumped mass within each bay.

(iii) The attenuation band-widths in torsion do not change significantly for inertia ratio greater than unity. This is also true in flexure with mass ratio exceeding one.

(iv) By proper choice of parameters within a feasible range, $(M+1)^{th}$ torsional propagation band can be entirely contained within the M^{th} bending propagation band. Perfect matching of these bands yield impractical values for the parameters involved.

(v) The entire flexural attenuation band can be made free from both bending and torsional resonances, and hence can be chosen as the operating speed range. This

range can be effectively increased by providing long (introducing rotational stiffness k_r), transversely flexible (introducing k_t) bearings.

REFERENCES

1. WILSON KER, W., Practical Solution of Torsional Vibration Problems, Vol. 1, Chapman and Hall, London, 1956.
2. BIEZENO, C.B. and GRAMMEL, R., Engineering Dynamics, Vol. 4, Blackie, London, 1953.
3. BISHOP, R.E.D. and JOHNSON, D.C., The Mechanics of Vibration, Cambridge University Press, Cambridge, 1960.
4. LEWIS, F.M., Vibration During Acceleration through a Critical speed, Transactions of the American Society of Mechanical Engineers, Vol. 54, pp. 253, 1932.
5. TIMOSHENKO, S. and YOUNG, D.H., Vibration Problems in Engineering, Van Mostrand, New York, 1955.
6. MALTBAEK, J.C., The Influence of a Discrete Inertia on the Free Torsional Vibrations of a Uniform Bar, International Journal of Mechanical Science, Vol. 4, pp. 25, 1962.
7. MALTBAEK, J.C., Torsional Vibration of a Stepped Shaft, Engineer, Vol. 223, pp. 972, 1967.
8. RAO, D.K., Torsional Frequencies of Multi-stepped Shaft with Rotors, International Journal of Mechanical Science, Vol. 20, pp. 415, 1978.
9. HECKL, M., Investigations on the Vibrations of Grillages and Other Simple Beam Structures, Journal of Accoustical Society of America, Vol. 36(7), pp. 1335, 1964.
10. HECKL, M., Wave Propagation in Beam-Plate Systems, Journal of Accoustical Society of America, Vol. 33, pp. 640, 1961.

11. MEAD, D.J., Free Wave Propagation in Periodically-Supported, Infinite Beams, Journal of Sound and Vibration, Vol. 11(2), pp. 181, 1970.

12. SENGUPTA, G., Natural Flexural Waves and the Normal Modes of Periodically-Supported Beams and Plates, Journal of Sound and Vibration, Vol. 13(1), pp. 89, 1970.

13. MEAD, D.J., Wave Propagation and Natural Modes in Periodic Systems: I. Mono-Coupled Systems, Journal of Sound and Vibration, Vol. 40(1), pp. 1-18, 1975.

14. MEAD, D.J., A General Theory of Harmonic Wave Propagation in Linear Periodic Systems with Multiple Coupling, Journal of Sound and Vibration, Vol. 27(2), pp. 235-260, 1973.

APPENDIX - A

MATRIX EQUATION FOR THE BOUNDARY CONDITIONS GIVEN BY EQUATIONS 2.29 (a-d)

$$\begin{bmatrix} 0 & 1 & 0 & 0 \\ 0 & 0 & -k_1 \sin k_1 & k_1 \cos k_1 \\ \cos k_1 \xi_1 & \sin k_1 \xi_1 & -\cos k_1 \xi_1 & -\sin k_1 \xi_1 \\ -k_1 \sin k_1 \xi_1 - I_D/I_s \cdot \Omega_s^2 \cdot \cos k_1 \xi_1 & k_1 \cos k_1 \xi_1 - I_D/I_s \cdot \Omega_s^2 \cdot \sin k_1 \xi_1 & k_1 \sin k_1 \xi_1 & -k_1 \cos k_1 \xi_1 \end{bmatrix} \begin{Bmatrix} A_1 \\ B_1 \\ A_2 \\ B_2 \end{Bmatrix} = \begin{Bmatrix} 1/K \\ 0 \\ 0 \\ 0 \end{Bmatrix} \quad \ldots\ldots (A.1)$$

From the above matrix equation, the constants A_1, B_1, A_2 and B_2 can be easily determined.

Similarly, when the non-dimensional torque at end B is unity, boundary conditions 2.29 (a) and (b) change to

$$\text{at} \quad \xi = 0 \qquad \theta'_L = 0$$

and

$$\text{at} \quad \xi = 1 \qquad \theta'_R = 1$$

Thus the right hand matrix in Eqn. A.1 gets modified to

$$\begin{Bmatrix} 0 \\ 1 \\ 0 \\ 0 \end{Bmatrix}$$

APPENDIX - B

MATRIX EQUATION FOR THE BOUNDARY CONDITIONS GIVEN BY EQUATION 2.33 (a-h)

$$
\begin{bmatrix}
+1 & 0 & +1 & 0 & 0 & 0 & 0 & 0 \\
0 & 0 & 0 & 0 & \cos k_2 & \sin k_2 & \cosh k_2 & \sinh k_2 \\
\cos k_2\xi_1 & \sin k_2\xi_1 & \cosh k_2\xi_1 & \sinh k_2\xi_1 & -\cos k_2\xi_1 & -\sin k_2\xi_1 & -\cosh k_2\xi_1 & -\sinh k_2\xi_1 \\
-k_2.\sin k_2\xi_1 & k_2.\cos k_2\xi_1 & k_2.\sinh k_2\xi_1 & k_2.\cosh k_2\xi_1 & k_2.\sin k_2\xi_1 & -k_2.\cos k_2\xi_1 & -k_2.\sinh k_2\xi_1 & -k_2.\cosh k_2\xi_1 \\
-k_2^2.\cos k_2\xi_1 & -k_2^2.\sin k_2\xi_1 & k_2^2.\cosh k_2\xi_1 & k_2^2.\sinh k_2\xi_1 & k_2^2.\cos k_2\xi_1 & k_2^2.\sin k_2\xi_1 & -k_2^2.\cosh k_2\xi_1 & -k_2^2.\sinh k_2\xi_1 \\
k_2^2 & \bar{k}_r.1/2.k_2 & -k_2^2 & \bar{k}_r.1/2.k_2 & 0 & 0 & 0 & 0 \\
0 & 0 & 0 & 0 & -k_2^2.\cos k_2 - (\bar{k}_r.1/2.k_2.\sin k_2) & -k_2^2.\sin k_2 + (\bar{k}_r.1/2.k_2.\cos k_2) & k_2^2.\cosh k_2 + (\bar{k}_r.1/2.k_2.\sinh k_2) & k_2^2.\sinh k_2 + (\bar{k}_r.1/2.k_2.\cosh k_2) \\
-\sin k_2\xi_1 - (M_D/M_b.k_2.\cos k_2\xi_1) & \cos k_2\xi_1 - (M_D/M_b.k_2.\sin k_2\xi_1) & -\sinh k_2\xi_1 - (M_D/M_b.k_2.\cosh k_2\xi_1) & -\cosh k_2\xi_1 - (M_D/M_b.k_2.\sinh k_2\xi_1) & \sin k_2\xi_1 & -\cos k_2\xi_1 & \sinh k_2\xi_1 & \cosh k_2\xi_1
\end{bmatrix}
\begin{Bmatrix} A_1 \\ B_1 \\ C_1 \\ D_1 \\ A_2 \\ B_2 \\ C_2 \\ D_2 \end{Bmatrix}
=
\begin{Bmatrix} 0 \\ 0 \\ 0 \\ 0 \\ 0 \\ - \\ 0 \\ 0 \end{Bmatrix}
$$

From the above matrix equation, the constants A_1 to D_1 and A_2 to D_2 are determined and the receptance β_{AA} is obtained as $\bar{W}'_A$.

Similarly, when unit non-dimensional moment (Ml/EI) is applied at end B, the boundary conditions 2.33 (f) and (g) change to :

$$\text{at } \xi = 0 \qquad -\bar{W}''_L + \frac{1}{2}.\bar{k}_r.\bar{W}'_L = 0$$

and $$\text{at } \xi = 1 \qquad \bar{W}''_R + \frac{1}{2}.\bar{k}_r.\bar{W}'_R = -1, \text{ respectively.}$$

Then the right hand matrix in Eqn. B.1 changes to

$$\begin{Bmatrix} 0 \\ 0 \\ 0 \\ 0 \\ 0 \\ 0 \\ -1 \\ 0 \end{Bmatrix}$$

A new set of values for the constants A_1-D_1 and A_2-D_2 are determined using the above right hand side matrix. Then the receptances β_{BB} and β_{AB} are obtained as $\bar{W}'_B$ and $\bar{W}'_A$ respectively.

APPENDIX - C

PROPAGATION CONSTANT IN TORSION

C-1 Propagation Constant for a Homogeneous Shaft

From the matrix equation of Appendix - A the constant A's and B's are evaluated for $I_D/I_s = 0.0$ and the receptances β_{AA} and β_{BA} are obtained as

$$\beta_{AA} = \theta_A = \frac{U_1 + U_2}{U_3 + U_4}$$

where $U_1 = -\frac{1}{k_1} \sin\frac{k_1}{2}(k_1 \sin\frac{k_1}{2} - k_1 \tan k_1 \cos\frac{k_1}{2})$

$$U_2 = +(\frac{I_D}{I_s}.k_1.\sin\frac{k_1}{2} - \cos\frac{k_1}{2})(\cos\frac{k_1}{2} + \sin\frac{k_1}{2}\tan k_1)$$

$$U_3 = \cos\frac{k_1}{2}(k_1 \sin\frac{k_1}{2} - k_1 \tan k_1 \cos\frac{k_1}{2})$$

$$U_4 = -(k_1 \sin\frac{k_1}{2} + \frac{I_D}{I_s}.k_1^2 \cos\frac{k_1}{2})(\cos\frac{k_1}{2} + \sin\frac{k_1}{2}\tan k_1)$$

and $\beta_{BA} = \theta_B = [1/\cos k_1][-1/(U_3 + U_4)]$

Hence, $\cosh\mu_t = \frac{\beta_{AA}}{\beta_{BA}} = \cos k_1 = \cos \Omega_s$

or, $\mu_{i,t} = |\Omega_s|$ (C.1)

C-2 Dependence of Propagation Constant on ξ

From the first set of boundary conditions (2.29(a-d)), where the torque is applied at end A, receptances β_{AA} and β_{BA} are found to be

$$\beta_{AA} = \Theta_A = [1 - \{\frac{I_D}{I_s}.k_1.\sin^2 k_1\xi\,(\cot k_1\xi + \tan k_1)\}]/$$

$$[k_1 \tan k_1 + \frac{I_D}{I_s}.k_1^2.\cos^2 k_1\xi(1+\tan k_1\xi \tan k_1)]$$

and $\beta_{BA} = \Theta_B = 1/[\cos k_1 \{ k_1 \tan k_1 + \frac{I_D}{I_s}.k_1^2.\cos^2 k_1\xi(1$

$+\tan k_1\xi \tan k_1)\}]$

Similarly from the second set of boundary conditions, when unit torque is applied at end B receptances β_{BB} and β_{AB} are obtained from appendix A, as

$$\beta_{BB} = \Theta_B = \frac{U_5}{U_6}$$

where $U_5 = [I_D/I_s.k_1.\cos^2 k_1\xi\,.\sec k_1(\sin k_1$

$+ \sin k_1 \tan k_1 \tan k_1\xi - \tan k_1\xi \sec k_1)] - 1$

$$U_6 = k_1 \tan k_1 + I_D/I_s.k_1^2.\cos^2 k_1\xi\,(1+\tan k_1\xi \tan k_1)$$

and $\beta_{AB} = \Theta_A = -1/[\cos k_1 \{ k_1 \tan k_1 + I_D/I_s.k_1^2.\cos^2 k_1\xi(1$

$+ \tan k_1\xi \tan k_1)\}]$

Substituting the above four receptance functions in Eqn. 2.10, it is seen that the torsional propagation constant, μ_t, can be obtained from

$$\cosh \mu_t = \frac{\beta_{BB} - \beta_{AA}}{2\beta_{AB}} = \cos \Omega_s - I_D/I_s.\frac{\Omega_s}{2}.\sin \Omega_s$$

So, the propagation constant, μ_t, is independent of ξ.

APPENDIX - D

EQUATIONS WITH TRANSVERSELY FLEXIBLE BEARINGS

As now there are two coupling co-ordinates at either end of every element, the system under consideration is a bi-coupled system. Shear force balance at both the ends gives

(i) at $\xi = 0$ $\quad \bar{W}_L''' / \bar{k}_t + \frac{1}{2} \bar{W}_L = 0$ (D.1)

(ii) at $\xi = 1$ $\quad -\bar{W}_R''' / \bar{k}_t + \frac{1}{2} \bar{W}_R = 0$ (D.2)

Continuity of displacement, slope and bending moment at $\xi = \xi_1$ gives

(iii) at $\xi = \xi_1$ $\quad \bar{W}_L = \bar{W}_R$ (D.3)

(iv) at $\xi = \xi_1$ $\quad \bar{W}_L' = \bar{W}_R'$ (D.4)

(v) at $\xi = \xi_1$ $\quad \bar{W}_L'' = \bar{W}_R''$ (D.5)

Non-dimensional bending moment (Ml/EI) at end A is unity

(vi) i.e. at $\xi = 0$ $\quad -\bar{W}_L'' + \frac{1}{2} \cdot \bar{k}_r \cdot \bar{W}_L' = 1$ (D.6)

Moment at end B is zero which gives

(vii) at $\xi = 1$ $\quad \bar{W}_R'' + \frac{1}{2} \cdot \bar{k}_r \cdot \bar{W}_R' = 0$ (D.7)

For the shear force balance at the mass

(viii) at $\xi = \xi_1$ $\quad -\bar{W}_L''' + \bar{W}_R''' = M_D / M_b \cdot \Omega_b^2 \cdot \bar{W}_L / R$ (D.8)

The (8x8) matrix equation resulting from the above boundary condition is as follows :

$$
\begin{bmatrix}
0.5 & -k_2^3/\bar{k}_t & 0.5 & k_2^3/\bar{k}_t & 0 & 0 & 0 & 0 \\
0 & 0 & 0 & 0 & \frac{-k_2^3 \cdot \sin k_2}{\bar{k}_t} & \frac{k_2^3 \cdot \cos k_2}{\bar{k}_t} & \frac{-k_2^3 \cdot \sinh k_2}{\bar{k}_t} & \frac{-k_2^3 \cdot \cosh k_2}{\bar{k}_t} \\
 & & & & +1/2 \cdot \cos k_2 & +1/2 \cdot \sin k_2 & +1/2 \cdot \cosh k_2 & +1/2 \cdot \sinh k_2 \\
\cos k_2\xi_1 & \sin k_2\xi_1 & \cosh k_2\xi_1 & \sinh k_2\xi_1 & -\cos k_2\xi_1 & -\sin k_2\xi_1 & -\cosh k_2\xi_1 & -\sinh k_2\xi_1 \\
-k_2 \cdot \sin k_2\xi_1 & k_2 \cdot \cos k_2\xi_1 & k_2 \cdot \sinh k_2\xi_1 & k_2 \cdot \cosh k_2\xi_1 & k_2 \cdot \sin k_2\xi_1 & -k_2 \cdot \cos k_2\xi_1 & -k_2 \cdot \sinh k_2\xi_1 & -k_2 \cdot \cosh k_2\xi_1 \\
-k_2^2 \cdot \cos k_2\xi_1 & -k_2^2 \cdot \sin k_2\xi_1 & k_2^2 \cdot \cosh k_2\xi_1 & k_2^2 \cdot \sinh k_2\xi_1 & k_2^2 \cdot \cos k_2\xi_1 & k_2^2 \cdot \sin k_2\xi_1 & -k_2^2 \cdot \cosh k_2\xi_1 & -k_2^2 \cdot \sinh k_2\xi_1 \\
k_2^2 & \bar{k}_r \cdot 1/2 \cdot k_2 & -k_2^2 & \bar{k}_r \cdot 1/2 \cdot k_2 & 0 & 0 & 0 & 0 \\
0 & 0 & 0 & 0 & -k_2^2 \cdot \cos k_2 & -k_2^2 \cdot \sin k_2 + & k_2^2 \cdot \cosh k_2 & k_2^2 \cdot \sinh k_2 \\
 & & & & -(\bar{k}_r \cdot 1/2 \cdot & (\bar{k}_r \cdot 1/2 \cdot & +(\bar{k}_r \cdot 1/2 \cdot & +(\bar{k}_r \cdot 1/2 \cdot \\
 & & & & k_2 \cdot \sin k_2) & k_2 \cdot \cos k_2) & k_2 \cdot \sinh k_2) & k_2 \cdot \cosh k_2) \\
-\sin k_2\xi_1 & \cos k_2\xi_1 & -\sinh k_2\xi_1 & -\cosh k_2\xi_1 & \sin k_2\xi_1 & -\cos k_2\xi_1 & \sinh k_2\xi_1 & \cosh k_2\xi_1 \\
-(M_D/M_b \cdot k_2 \cdot & -(M_D/M_b \cdot k_2 \cdot & -(M_D/M_b \cdot k_2 \cdot & -(M_D/M_b \cdot k_2 \cdot & & & & \\
\cos k_2\xi_1) & \sin k_2\xi_1) & \cosh k_2\xi_1) & \sinh k_2\xi_1) & & & &
\end{bmatrix}
\begin{Bmatrix} A_1 \\ B_1 \\ C_1 \\ D_1 \\ A_2 \\ B_2 \\ C_2 \\ D_2 \end{Bmatrix}
=
\begin{Bmatrix} 0 \\ 0 \\ 0 \\ 0 \\ 0 \\ 1 \\ 0 \\ 0 \end{Bmatrix}
$$

In this analysis, the receptance equations given in Chapter 2 for a mono-coupled system, are modified as :

$$\begin{aligned}
\Theta_A &= \beta_{AA} M_A + \beta_{AB} M_B + \gamma_{AA} F_A + \gamma_{AB} F_B \\
\Theta_B &= \beta_{BA} M_A + \beta_{BB} M_B + \gamma_{BA} F_A + \gamma_{BB} F_B \\
\overline{W}_A &= \delta_{AA} M_A + \delta_{AB} M_B + \alpha_{AA} F_A + \alpha_{AB} F_B \\
\overline{W}_B &= \delta_{BA} M_A + \delta_{BB} M_B + \alpha_{BA} F_A + \alpha_{BB} F_B
\end{aligned} \qquad \text{(D.10)}$$

where β_{ij} is the harmonic rotation at i to unit harmonic moment at j,

γ_{ij} is the harmonic rotation at i due to unit harmonic force at j, δ_{ij} is the harmonic deflection at i due to unit harmonic moment at j, and α_{ij} is the harmonic deflection at i due to unit harmonic force at j.

Four sets of receptance functions, namely, $[\beta_{AA}, \beta_{BA}, \delta_{AA}$ and $\delta_{BA}]$; $[\beta_{AB}, \beta_{BB}, \delta_{AB}$ and $\delta_{BB}]$; $[\gamma_{AA}, \gamma_{BA}, \alpha_{AA}$ and $\alpha_{BA}]$ and $[\gamma_{AB}, \gamma_{BB}, \alpha_{AB}$ and $\alpha_{BB}]$ are obtained respectively by four sets of boundary conditions which are resulted by the application of unit moment and unit force, respectively, at each end. The resulting four right hand column matrices are as follows:

Unit moment about A	Unit moment about B	Unit shear force at A	Unit shear force at B
0	0	$-1/\bar{k}_t$	0
0	0	0	$1/\bar{k}_t$
0	0	0	0
0	0	0	0
0	0	0	0
1	0	0	0
0	-1	0	0
0	0	0	0